



## Research paper

## Novel indolo-sophoridinic scaffold as Topo I inhibitors: Design, synthesis and biological evaluation as anticancer agents

Yiming Xu<sup>a,1</sup>, Lichuan Wu<sup>b,1</sup>, Haroon Ur Rashid<sup>a,c</sup>, Dewang Jing<sup>a</sup>, Xiaole Liang<sup>d</sup>, Haodong Wang<sup>a</sup>, Xu Liu<sup>b</sup>, Jun Jiang<sup>a</sup>, Lisheng Wang<sup>b,\*</sup>, Peng Xie<sup>a,\*\*</sup><sup>a</sup> School of Chemistry and Chemical Engineering, Guangxi University, Nanning, 530004, China<sup>b</sup> Medical College, Guangxi University, Nanning, 530004, China<sup>c</sup> Department of Chemistry, Sarhad University of Science & Information Technology, Peshawar, Khyber Pakhtunkhwa, 25120, Pakistan<sup>d</sup> Laboratory of Basic Medicine, Guangxi Medical University Nanning, 530022, China

## ARTICLE INFO

## Article history:

Received 22 May 2018

Received in revised form

27 June 2018

Accepted 10 July 2018

## Keywords:

Indolo-sophoridinic Topo I inhibitors

Molecular docking

Binding mode

Anticancer activities

Enzymatic activity

## ABSTRACT

Based on the mechanism of action, novel scaffolds as Topo I inhibitors bearing indole and sophoridine were designed. Preliminary docking study revealed that some molecules among the designed series possessed promising Topo I inhibitor properties. Subsequently, thirty new compounds were synthesized and characterized by <sup>1</sup>H NMR, <sup>13</sup>C NMR, and Mass spectral analyses. The compounds were then screened for their antiproliferative and enzymatic inhibitory activities. The results affirmed the consistency between docking and activities and the rationality of the design strategy. Furthermore, compound **10b** was chosen as a representative compound to test its anticancer effects *in vitro* and *in vivo*. The results showed that **10b** caused prominent S phase cell cycle arrest and significantly suppressed tumor growth in HepG2 cell derived mouse model. These findings present a promising series of lead molecules which can serve as potential Topo I inhibitors for the treatment of cancer and a theoretical basis for structural modifications.

© 2018 Published by Elsevier Masson SAS.

## 1. Introduction

DNA topoisomerase I (Topo I) is an essential and ubiquitous enzyme that cleaves a single DNA strand to relax supercoiled DNA for replication, transcription, recombination, and chromatin remodeling [1–3]. Topo I is over-expressed in many cancer types and can promote cancer cell proliferation [4–7]. Thus, Topo I is recognized as important target in cancer therapy and anticancer drug design. Therefore, developing new Topo I inhibitors has become a hotspot research in medicinal chemistry.

Presently, the studies on Topo I inhibitors have focused on alkaloids, among which camptothecins are the primary Topo I inhibitors. Despite of their potent anticancer activity, many limitations could be well-defined in all of the camptothecins [8,9]. In addition to their dose-limiting toxicity, camptothecins are inactivated within minutes at physiological PH due to their

transformation to camptothecin carboxylate by lactone E ring opening [10–12]. Thus, development of Topo I inhibitors with new scaffold can be expected to overcome these shortcomings. Indolo-carbazoles, indenoisoquinolines, and dibenzonaphthridinones represent a class of non-camptothecins compounds which have been reported to possess the most extensive applications as Topo I inhibitors (Fig. 1) [13–17].

An evident feature of the above poisons is their planar heterocyclic ring structure containing nitrogen. A comparative analysis of three different ternary structures obtained via X-ray crystal structure models indicates that camptothecin, indolocarbazole, and indenoisoquinoline compounds are bound to the topoisomerase I-DNA complex, and further reveals some prominent resemblance on the mode of action of the Topo I poisons. The characteristic structures of these poisons allow them to intercalate into DNA and form stacking interactions with base pairs by mimicking a DNA base pair. It is vital to mention that most of the solvent accessible part of every compound is protected by DNA (57%–70%) due to intercalation binding mode, which further supports the idea that stacking interactions may be the primary binding interaction for these Topo I poisons [18] (Fig. 2). Thus, it is necessary to design new drug

\* Corresponding author.

\*\* Corresponding author.

E-mail addresses: [lswang@gxu.edu.cn](mailto:lswang@gxu.edu.cn) (L. Wang), [xiep@gxu.edu.cn](mailto:xiep@gxu.edu.cn) (P. Xie).<sup>1</sup> These authors have contributed equally.

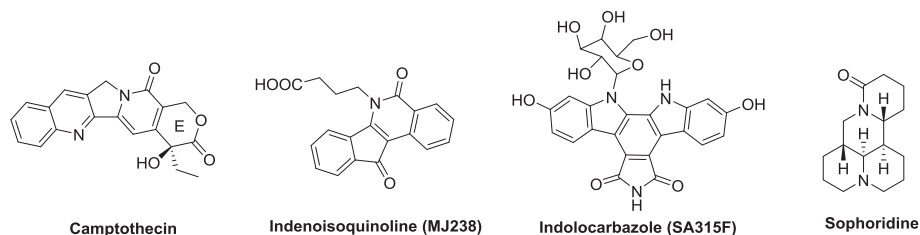


Fig. 1. Structures of camptothecin, indenoisoquinoline, indolocarbazole and sophoridine.

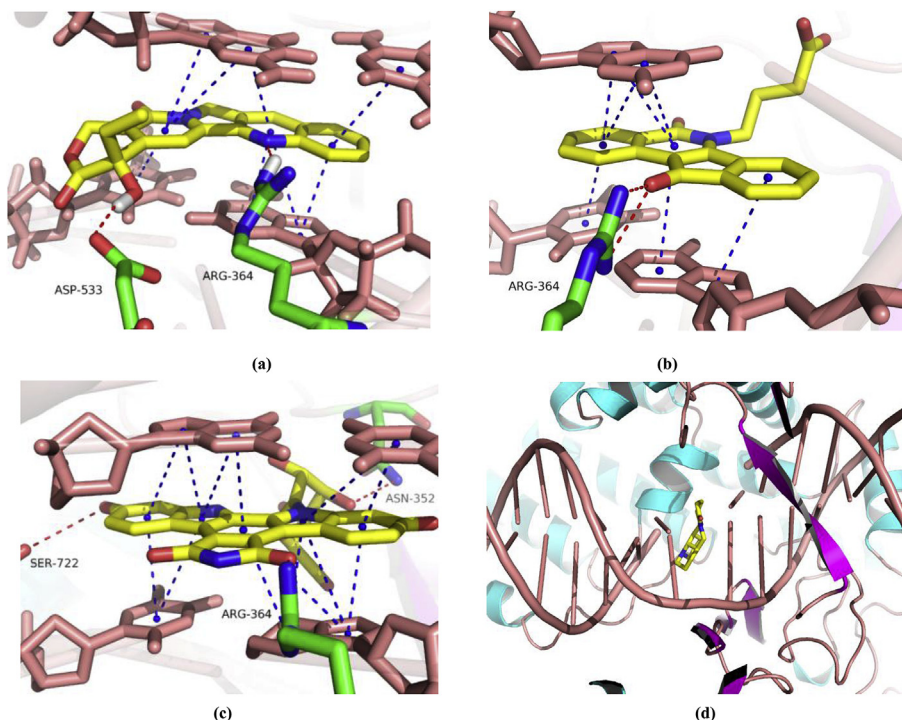


Fig. 2. The binding mode of Camptothecin (a), Indenoisoquinoline (b), Indolocarbazole (c) with Topo I-DNA complex obtained via X-ray crystal structure models and the binding mode of Sophoridine (d) with Topo I gained via molecular docking.

skeleton bearing planar heterocyclic ring to perform  $\pi$ - $\pi$  stacking interactions with DNA. Besides, the study also reveals that the poisons can take effect at high concentrations and thus cause dose-limiting toxicities which in turn can damage normal tissues. So, in addition to the planar heterocyclic ring mentioned above, another moiety in newly designed scaffold that expected to render the drugs with effects of improved metabolism, bioavailability and better pharmacological profile should also be contained.

Sophoridine, another Topo I inhibitor, has captured our attention due to its several druggable advantages such as special chemical scaffold, flexible structure, high solubility, and good safety profiles compared to other Topo I inhibitors referred above [19–22]. However, the moderate antitumor activity of sophoridine limits its use as a single drug for clinical applications. Therefore, it is reasonable to develop more effective drug candidates based on sophoridinic structure [23–25]. The binding mode of sophoridine revealed that sophoridine only interacted with Topo I rather than DNA (Fig. 2). The aforementioned evidences provide mechanistic foundations for the combination of planar heterocyclic ring with sophoridine. When the new Topo I inhibitors contained the two moieties, it may help to stabilize the covalent enzyme-DNA complex by enhancing base stacking interaction and confer a number of physiological and pharmaceutical activities in cancer therapy. In

this study, we intended to develop Topo I inhibitors based on the rational drug design strategy.

## 2. Rational design of Topo I inhibitors

Indole, widely distributed in natural products, is a simple molecule bearing bicyclic planar constructions and has similarities with camptothecin, indolocarbazole, and indenoisoquinoline compounds. In addition, it is a key component in the skeletal structure of several well-known drugs [26,27] and indole derivatives have wide spectrum of biological activities, including antituberculosis [28], anti-inflammatory [29,30], antitumor [31,32], anticonvulsion and anticardiovascular effects [33,34]. We speculated that indole as a necessary moiety of inhibitors which could intercalate into DNA and interact with Topo I. Therefore, indole was chosen for the synthesis of inhibitors. The simple and small structure of sophoridine provides advantages in chemical synthesis and offers opportunities of formulation for oral administration. Besides, its structure-activity relationship reveals that sophoridinic acid analogues containing a 3-ring core scaffold are more favorable than sophoridine containing a 4-ring scaffold ring [35]. So the ring D of sophoridine was opened and the resultant product was allowed to combine with indole skillfully at

3-position through Mannich reaction, which also provides us an opportunity to perform further substitution at N-position of indole moiety and side chain of sophoridinic acid. Consequently, preliminarily docking studies of a series of preconceived indolo sophoridinic derivatives were performed with the Topo I target and then the desired products were synthesized and evaluated for their anticancer activity (Scheme 1).

### 3. Results and discussion

#### 3.1. Molecular docking

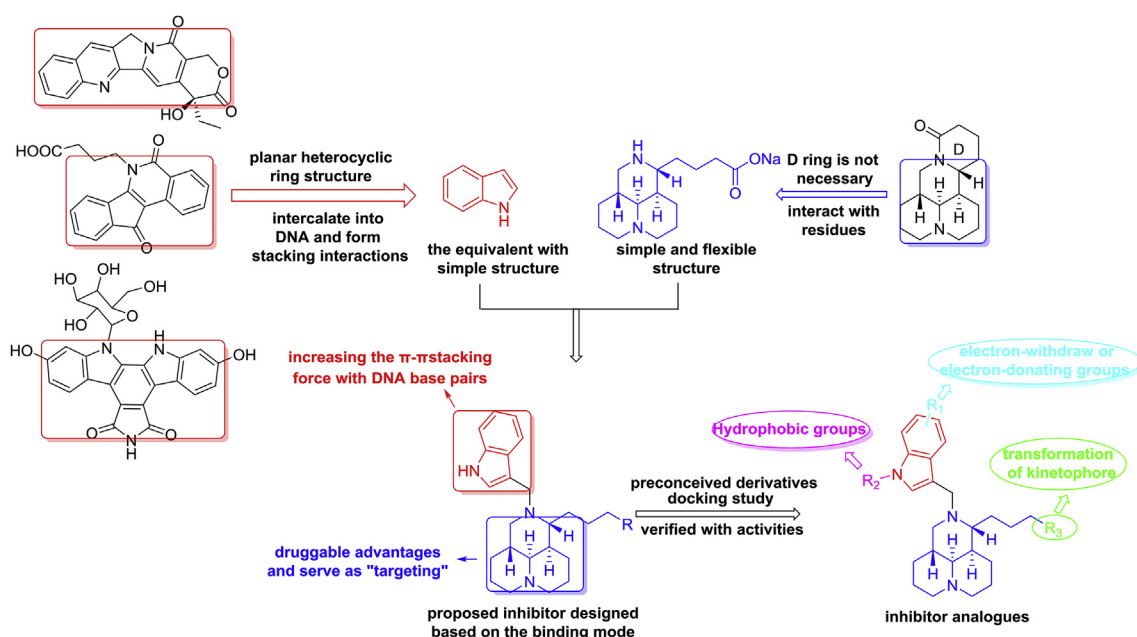
Molecular docking was first performed on proposed inhibitor **4a** with DNA Topo I complex. As we predicted, the docking score of **4a** is much better than sophoridine, indicating that the introduced indole moiety could significantly improve affinity with Topo I. We speculated that the primary affinity between indole moiety and Topo I is the base-stacking force caused by the  $\pi$ - $\pi$  electron interaction with the base, which could stabilize the DNA helix structure. To further understand the influence of the stacking force caused by the electron density, docking of **4d-4f** bearing electrophilic groups and **4b-4c** carrying electron-donating groups with Topo I was performed after variation of R<sub>1</sub> at 5-position. Among the compounds, **4b** and **4f** exhibited potent docking score. While considering the importance of halides in the drug designing research, compounds **4g-4j** containing a variety of halogens at different positions on the indole moiety were chosen for docking. Due to the importance of alkylation strategy in drug design and modification, a variety of alkyl groups were introduced on the nitrogen atom and docking was executed. Better docking results of **6a-6d** than **4a** revealed that alkyl group could enhance the activity. Concurrently, docking of compounds **6e-6p** with a variety of aryl groups was also performed. Hydrophobicity, as a fundamental pharmacological parameter, could influence the absorption of medicine, biological activities, interactions with receptors and the toxicity from molecular metabolism etc. Herein, the ester group was transformed into alcohol and carboxyl functionality and docking results of the derivatives were also obtained (Table 1).

#### 3.2. Chemistry

The docking results suggest that targeting newly designed inhibitor is a promising strategy for cancer therapy (Table 1). To verify the possibility of the strategy, thirty novel N-substituted indolo sophoridinic acid derivatives (mentioned above) were synthesized (Scheme 2) using commercially available **1** as a starting material. The desired product **2** was prepared via hydrolysis of **1** in aqueous NaOH at the reflux temperature, which was then reacted with sulfoxide chloride and alcohol to produce product **3**. The iminium intermediate was prepared by the addition of **3** to formaldehyde in the presence of acetic acid which was subsequently reacted with various indolo substituents to produce **4a-4e** skillfully by Mannich reaction. A series of halohydrocarbon acted as alkylating agents to synthesize **6a-6e** from **4a-4e** using K<sub>2</sub>CO<sub>3</sub> as a base. Similarly, the desired compounds **6a-6e** could also be produced through the reaction of **3** with N-substituted indolo derivatives (**5a-5e**) directly. Finally, considering the influence of pharmacology on hydrophobicity, the study of structure activity relationship was focused on the side chain. The ester functionality of compounds **4a**, **6e** and **6j** was transformed into alcohol group resulting in the formation of compounds **9**, **10a** and **10b** respectively. Compound **2** was also tried to transform to compound **11**. However, the structure of compound **11** is unstable and its instability is suspected to be caused by amino and carboxyl groups with different pH values. In this work, high reaction yield is observed in each step, which provides the feasibility of a useful application in terms of synthesis and drug development cost. Melting points of the newly synthesized compounds were determined by X-4 melting point apparatus. Their structures were characterized by <sup>1</sup>H NMR, <sup>13</sup>C NMR and high resolution ESI-MS spectra.

#### 3.3. MTT assays

The target compounds were tested for their cytotoxic activities in HepG2, CNE-2 and A549 cell lines with camptothecin as the positive control using MTT assays. Structures of derivatives and their cytotoxic activities are shown in Table 2.



Scheme 1. Design strategy for Topo I inhibitors.

**Table 1**  
Docking results of the derivatives with Topo I -DNA complex (PDB: 1T8I).

Ligand	Docking score <sup>a</sup>	Glide energy <sup>b</sup>	Lipophilic EvdW <sup>c</sup>	Hbond <sup>d</sup>	Glide emodel <sup>e</sup>
Sophoridine	-3.294	-19.341	-2.656	0	-29.277
4a	-5.778	-46.323	-5.687	0	-68.591
4b	-6.58	-52.238	-5.74	-0.786	-77.767
4c	-5.415	-53.741	-4.769	-0.347	-71.203
4d	-5.518	-50.663	-5.202	-0.35	-67.064
4e	-4.716	-56.465	-4.573	0	-78.233
4f	-6.383	-50.332	-5.896	-0.35	-74.477
4g	-5.705	-43.801	-4.55	-0.807	-69.349
4h	-5.959	-48.354	-5.909	0	-67.644
4i	-4.154	-45.261	-3.844	-1.041	-66.654
4j	-4.171	-45.222	-3.681	-0.981	-66.001
4k	-6.878	-58.222	-6.1	-0.574	-80.574
6a	-6.254	-48.926	-6.195	0	-71.272
6b	-6.421	-45.491	-5.667	-0.7	-71.332
6c	-4.324	-51.874	-6.846	-1.379	-80.947
6d	-6.928	-50.881	-6.06	-0.7	-79.884
6e	-8.151	-57.906	-8.037	-0.156	-91.192
6f	-6.725	-56.413	-5.93	-0.7	-89.064
6g	-7.497	-60.511	-6.773	-0.495	-91.741
6h	-6.841	-59.616	-6.225	-0.367	-89.282
6i	-6.833	-57.156	-6.749	0	-91.902
6j	-7.774	-58.986	-7.145	-0.35	-96.019
6k	-6.863	-59.798	-7.068	0	-96.922
6l	-6.659	-64.477	-6.141	-1.056	-96.667
6m	-6.977	-62.288	-6.766	-0.35	-103.263
6n	-7.423	-60.84	-6.771	-1.043	-100.655
6o	-4.756	-53.887	-3.826	-1.361	-82.305
6p	-4.331	-57.421	-5.248	-0.012	-88.986
7	-6.801	-46.036	-5.082	-1.33	-61.908
10a	-6.887	-51.316	-6.164	-0.722	-83.008
10b	-7.521	-57.519	-7.212	-0.35	-91.003
11	-4.324	-51.874	-6.846	-1.379	-80.947
Camptothecin	-8.901	-62.819	-7.668	-0.48	-92.869

<sup>a</sup> Docking score, including terms in the scoring function, various indexes, and ligand efficiency metrics, rank the affinity of ligands bound to the active site of a receptor.

<sup>b</sup> Glide energy, revealing the Modified Coulomb-van der Waals interaction energy.

<sup>c</sup> Lipophilic EvdW, indicating Lipophilic term derived from hydrophobic grid potential at the hydrophobic ligand atoms.

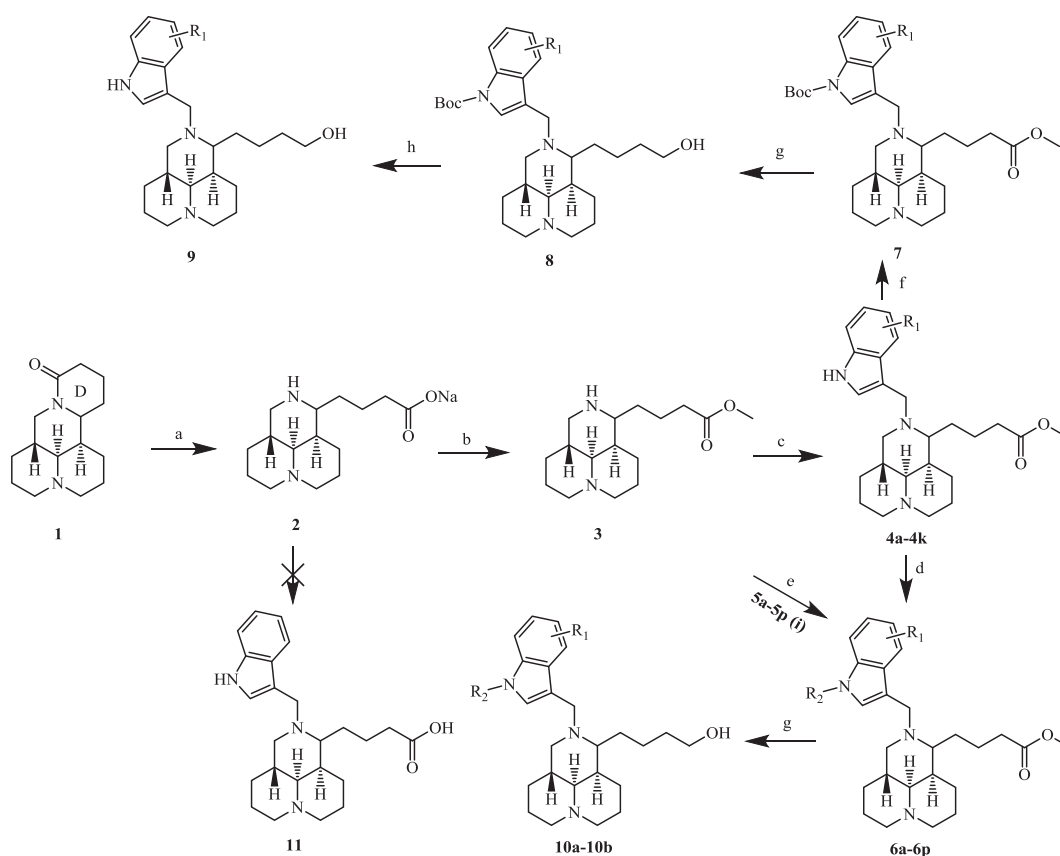
<sup>d</sup> Hbond, Hydrogen-bonding term. This term is separated into differently weighted components that depend on whether the donor and acceptor are neutral, one is neutral and the other is charged, or both are charged.

<sup>e</sup> Glide emodel, indicating model energy. Emodel combines GlideScore, the nonbonded interaction energy, and, for flexible docking, the excess internal energy of the generated ligand conformation.

Indole moiety was firstly introduced to sophoridine to produce compound **4a**. The cytotoxic activities results confirmed more potent activities of compound **4a** than sophoridine against three cancer cell lines, indicating indole moiety significantly enhanced the anticancer activity. Besides, the docking score of **4a** (with -5.778) is better than that of sophoridine (with -3.294) (Table 2). These results verified the rationality of the strategy, turning the activity from millimole into a micromole. The drugs were designed to enhance the anticancer activity by stabilizing the DNA-Topo I complex, in which the primary affinity is the base stacking force caused by the interaction between  $\pi$  electrons derived from indole moiety and base pairs. Therefore, it was imperative to focus the structure activity analysis on the electron cloud of indole moiety. With a variety of indole structures bearing electron-withdrawing and electron-donating groups introduced into sophoridine, compounds **4a-4k** were obtained and the influence on the bioactivity caused by the electronic cloud distribution on the indole moiety was explored. The results showed that the activities of all the derivatives of **4a** (obtained after substitution at R<sub>1</sub>) were poorer than the parent compound **4a** itself. This led us to the conclusion that the increase and decrease of the  $\pi$  electron cloud induced by electronic effect on the indole moiety could weaken the base stacking force. We speculated that electron distribution on indole moiety without R<sub>1</sub> substituents was the most favorable condition for improving  $\pi$ - $\pi$  interaction furthest.

However, as illustrated in Table 1, not all the **4a-4k** docking

scores were in accordance with the activity result. Among the compounds, **4b**, **4f**, **4h**, and **4k** bear better score (-6.58, -6.383, -5.959 and -6.878 respectively) than **4a** (-5.778), while **4a** exhibited better activity than these compounds. We conjectured that docking could simulate and predict the binding mode of  $\pi$ - $\pi$  interaction between ligands and acceptor, but it is difficult to estimate the impact of changing electron cloud distribution on the affinity, leading to the diversity between calculation and experiment. Next, we introduced a variety of alkyl and aryl groups on the nitrogen atom at the 1-position of indole. Compounds **6a-6d** and **6e-6m** were synthesized and investigated. Majority of these compounds exhibited better anticancer activities than **4a**. Meanwhile, the docking score exerted high consistency with the activity indicating that alkyl and aryl groups play an important role in improving the activity and feasibility of guidance by docking. More importantly, the mechanism might be explained by the use of the calculated docking data. As shown in Table 1, the Lipophilic EvdWc parameter is closely related to the docking score, the introduced alkyl and aryl groups lowered the glide energy by decreasing the Lipophilic EvdWc, and thus enhanced the activity. Besides, by comparing the activity results of **6i**, **6k**, and **6l** with **6n**, **6o** and **6p**, it is obvious that the existence of fluorine atom reduced the activity, also indicated that variation in electron density had disadvantage for stacking force. On the other hand, **6o** and **6p** perform better activity than **4a**, however, their docking score (-4.756, -4.331) is not as good as that of **4a** (-5.778), making it difficult once again to



**Scheme 2.** Reagents and conditions: (a) NaOH aqueous, reflux, 8h; (b) SOCl<sub>2</sub>, MeOH, reflux, 3h; (c) HCHO, AcOH, R<sub>1</sub> bearing indolo derivatives, H<sub>2</sub>O or CHCl<sub>3</sub>, rt; (d) NaH, halides, DMSO, rt; (e) HCHO, AcOH, **5a-5p**, H<sub>2</sub>O or CHCl<sub>3</sub>, rt; (f) (Boc)<sub>2</sub>O, TEA, CH<sub>2</sub>Cl<sub>2</sub>, rt, 5h; (g) LiAlH<sub>4</sub>, THF, rt, 2h; (h) NaHSO<sub>4</sub>·SiO<sub>2</sub>, CH<sub>2</sub>Cl<sub>2</sub>, reflux; (i) R<sub>1</sub> bearing indolo derivatives, Halides with R<sub>2</sub> group, DMF, NaH, rt.

predict the dependency of the stacking force influence on the altering electron cloud. Finally, alcohols (**7**, **10a** and **10b**) with improved water solubility were obtained, aiming to execute the SAR exploration on the effect caused by metabolism and stability. The results revealed that a variation existed in the activities when the functional group transformed from ester to alcohol. Compound **10a** exhibited better activities than **6e** against HepG2, CNE-2 and A549, whereas **10b** showed poorer activities than **6j** against A549, indicating that the alcohol group did not make positive contribution to all compounds. Thus, these results provided important clue for designing new inhibitors.

Based on the feasibility of docking results and the binding mode of camptothecin, indolocarbazole, indenoisoquinoline and sophoridine the proposed inhibitor **4a** was designed first. Then a series of **4a** derivatives was constructed by docking and their bioactivities were verified. Overall, the docking and activity results simultaneously revealed that indole is a necessary moiety for the inhibitors and the introduction of alkyl and aryl groups could improve the activity to some degree. These findings showed a correlation between biological activity and docking. Although limitation existed and was confirmed, the analysis preliminarily verified the rationality of design. Further verification was carried out by enzymatic activity.

#### 3.4. Topo I inhibitory activity

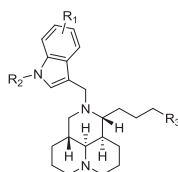
To verify the rational design and explore the mechanism by which compounds inhibited Topo I and thereby caused cytotoxicity, fourteen compounds were examined at 500 μM by measuring the

relaxation of supercoiled DNA of plasmid pBR322 with CPT as positive control (Fig. 3) [36]. The results showed that compounds **6e**, **6i**, **6m**, **10a** and **10b** (with good docking score: −8.151, −6.833, −6.977, −6.887, −7.521 respectively) could inhibit the enzymatic activity, which are basically consistent with the docking score, further indicating the rationality of the design strategy. It is noteworthy that compound **10b** exhibited potent inhibitory activity against Topo I and antiproliferative activity against tested cancer cell lines simultaneously. Thus, **10b** was chosen for further investigation.

#### 3.5. Docking analysis of **10b** with Topo I-DNA complex

Based on above study results, **10b** was chosen as a representative for molecular docking studies in order to further understand the binding modes of the analogues (Fig. 4). The indole rings in **10b** mimic a DNA base pair and thereby form stacking interactions with both upstream and downstream base pairs DT10 and TGP11, respectively. On the other hand, the sophoridinic moiety of **10b** formed hydrogen bonds with residues LYS436. Furthermore, the 4-bromobenzyl substituent of **10b** could not only form Lipophilic EvdW interaction but can also produce π-π stacking force with base pairs DA113 and DC112 similar to indole moiety, thus contributing to the overall interaction. It explains why the introduction of various benzyl groups could enhance the activities. In summary, the above molecular simulations give us rational explanation of the interactions between ligand **10b** and DNA-Topo I, which in turn provided valuable information for further development of DNA-Topo I inhibitors.

**Table 2**  
Structures and the *in vitro* cytotoxic activities of target derivatives.



Compound	R <sub>1</sub>	R <sub>2</sub>	R <sub>3</sub>	IC <sub>50</sub> ( $\mu$ M) <sup>a</sup>		
				HepG2	CNE-2	A549
Sophoridine	/	/	/	4670 $\pm$ 127	5379 $\pm$ 109	5836 $\pm$ 97
4a	H	H	COOCH <sub>3</sub>	36.5 $\pm$ 1.8	12.1 $\pm$ 1.6	27.8 $\pm$ 2.3
4b	5-CH <sub>3</sub>	H	COOCH <sub>3</sub>	23.8 $\pm$ 2.5	49.4 $\pm$ 2.2	>50
4c	5-OCH <sub>3</sub>	H	COOCH <sub>3</sub>	>50	>50	>50
4d	5-CN	H	COOCH <sub>3</sub>	>50	15.3 $\pm$ 1.5	>50
4e	5-NO <sub>2</sub>	H	COOCH <sub>3</sub>	>50	>50	>50
4f	5-Cl	H	COOCH <sub>3</sub>	>50	17.9 $\pm$ 1.7	>50
4g	5-Br	H	COOCH <sub>3</sub>	31.8 $\pm$ 3.4	20.2 $\pm$ 3.1	39.9 $\pm$ 3.8
4h	5-F	H	COOCH <sub>3</sub>	>50	>50	>50
4i	4-F	H	COOCH <sub>3</sub>	>50	>50	>50
4j	6-F	H	COOCH <sub>3</sub>	>50	17.1 $\pm$ 2.1	>50
4k	2-COOCH <sub>3</sub>	H	COOCH <sub>3</sub>	>50	26.4 $\pm$ 3.1	>50
6a	H	CH <sub>3</sub>	COOCH <sub>3</sub>	15.2 $\pm$ 1.2	43.4 $\pm$ 2.6	42.8 $\pm$ 3.4
6b	H	CH <sub>2</sub> CH <sub>3</sub>	COOCH <sub>3</sub>	12.8 $\pm$ 1.9	19.4 $\pm$ 1.2	37.4 $\pm$ 3.6
6c	H	CH <sub>2</sub> CH <sub>2</sub> CH <sub>2</sub> CH <sub>3</sub>	COOCH <sub>3</sub>	6.2 $\pm$ 0.8	8.6 $\pm$ 1.8	42.8 $\pm$ 2.3
6d	H		COOCH <sub>3</sub>	14.4 $\pm$ 1.0	13.4 $\pm$ 2.4	30.3 $\pm$ 3.3
6e	H	CH <sub>2</sub> C <sub>6</sub> H <sub>5</sub>	COOCH <sub>3</sub>	5.5 $\pm$ 0.6	3.3 $\pm$ 0.9	43.4 $\pm$ 3.2
6f	H	CH <sub>2</sub> C <sub>6</sub> H <sub>4</sub> F- <i>o</i>	COOCH <sub>3</sub>	21.7 $\pm$ 1.3	14.8 $\pm$ 2.3	49.3 $\pm$ 2.4
6g	H	CH <sub>2</sub> C <sub>6</sub> H <sub>4</sub> F- <i>m</i>	COOCH <sub>3</sub>	12.1 $\pm$ 2.6	12.1 $\pm$ 1.2	42.3 $\pm$ 5.4
6h	H	CH <sub>2</sub> C <sub>6</sub> H <sub>4</sub> F- <i>p</i>	COOCH <sub>3</sub>	8.6 $\pm$ 3.1	3.5 $\pm$ 1.2	29.6 $\pm$ 1.3
6i	H	CH <sub>2</sub> C <sub>6</sub> H <sub>4</sub> Cl- <i>p</i>	COOCH <sub>3</sub>	6.5 $\pm$ 2.7	4.6 $\pm$ 1.4	5.2 $\pm$ 1.6
6j	H	CH <sub>2</sub> C <sub>6</sub> H <sub>4</sub> Br- <i>p</i>	COOCH <sub>3</sub>	4.8 $\pm$ 1.6	4.3 $\pm$ 0.7	3.5 $\pm$ 0.8
6k	H	CH <sub>2</sub> C <sub>6</sub> H <sub>4</sub> CF <sub>3</sub> - <i>p</i>	COOCH <sub>3</sub>	6.1 $\pm$ 1.3	4.8 $\pm$ 0.8	7.4 $\pm$ 0.9
6l	H		COOCH <sub>3</sub>	8.5 $\pm$ 1.4	6.7 $\pm$ 1.4	3.7 $\pm$ 0.5
6m	H		COOCH <sub>3</sub>	8.6 $\pm$ 2.1	7.8 $\pm$ 1.2	24.0 $\pm$ 1.8
6n	5-F	CH <sub>2</sub> C <sub>6</sub> H <sub>4</sub> Cl- <i>p</i>	COOCH <sub>3</sub>	7.3 $\pm$ 1.0	6.1 $\pm$ 2.0	10.6 $\pm$ 3.4
6o	5-F	CH <sub>2</sub> C <sub>6</sub> H <sub>4</sub> CF <sub>3</sub> - <i>p</i>	COOCH <sub>3</sub>	7.7 $\pm$ 0.7	6.9 $\pm$ 1.0	12.8 $\pm$ 1.5
6p	5-F		COOCH <sub>3</sub>	18.4 $\pm$ 3.3	9.3 $\pm$ 1.5	39.8 $\pm$ 1.8
7	H	H	CH <sub>2</sub> OH	>50	>50	>50
10a	H	CH <sub>2</sub> C <sub>6</sub> H <sub>5</sub>	CH <sub>2</sub> OH	2.3 $\pm$ 0.6	2.2 $\pm$ 0.7	33.7 $\pm$ 2.4
10b	H	CH <sub>2</sub> C <sub>6</sub> H <sub>4</sub> Br- <i>p</i>	CH <sub>2</sub> OH	3.1 $\pm$ 0.8	3.5 $\pm$ 1.3	22.1 $\pm$ 3.5
camptothecin	/	/	/	13.2 $\pm$ 2.6	0.1 $\pm$ 0.04	5.5 $\pm$ 0.7

<sup>a</sup> Data are expressed as the mean  $\pm$  SD of at least three independent experiments.

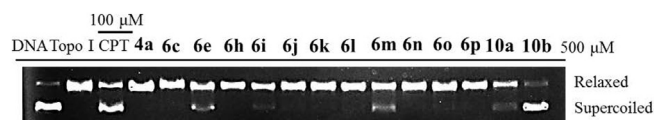


**Fig. 3.** Topo I inhibitory activities. lane DNA, pBR322 DNA; lane Topo I, Topo I + pBR322 DNA; lane CPT: camptothecin (100  $\mu$ M) + Topo I + pBR322 DNA; the others: various derivatives (500  $\mu$ M) + Topo I + pBR322 DNA.

From an overall perspective, the special structure of parent sophoridine offers many pharmacological advantages such as simple chemical scaffold, flexibility, high solubility, and good safety profiles to the new inhibitors. More significantly, as illustrated in the binding mode, the structure could serve as a target carrier for the planner indole moiety, conveyed to the DNA active site and

showing a pronounced effect. On the other hand, it is obvious that the primary binding force between ligands and DNA-Topo I is the base stacking force produced by the  $\pi$ - $\pi$  interaction from indole moiety and DNA base upstream and downstream. The design strategy could clearly be described by the mode and it can mutually be argued with the experiment. The strategy provides useful information for designing better new Topo I inhibitors with bigger planner heteroaromatic ring, connecting it with sophoridine scaffold bearing more druggable advantages.

### 3.6. Cell cycle analysis

It is reported that cytotoxicity of Topo I inhibitor depended on active DNA replication [37]. Based on compound **10b** showing positive activity in MTT assay and Topo I inhibition assay, we

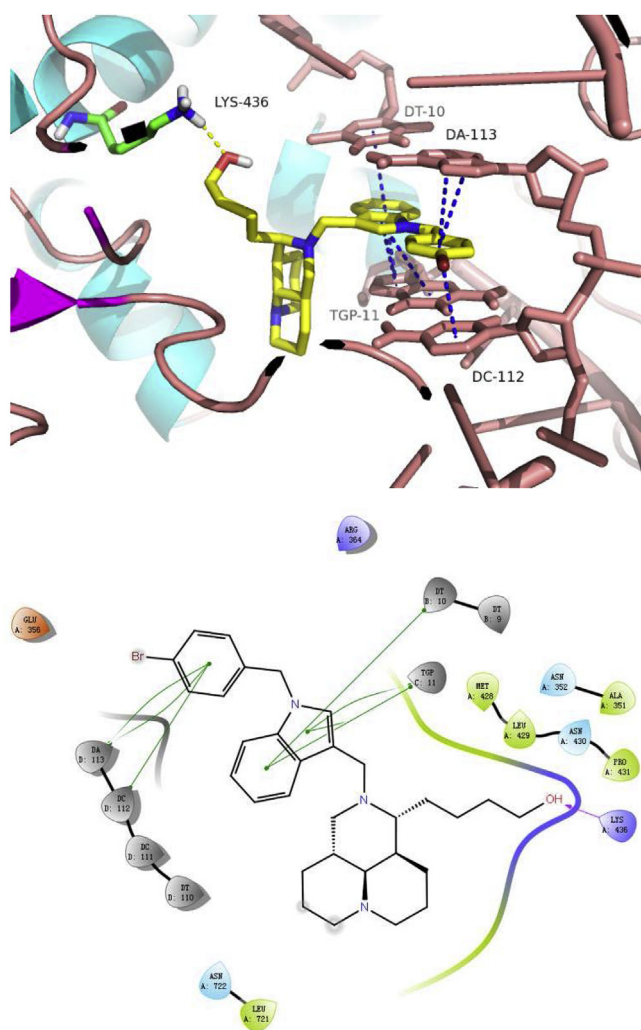


Fig. 4. The binding mode of compound 10b with Topo I-DNA complex.

further investigated the effect of **10b** on cell cycle distribution. The results indicated that compound **10b** led to S phase cell cycle arrest. In fact, after 24 h, the cell population in S increases from 45.44% in the untreated cells to 55.77%, 60.68% and 64.17% in the cells treated with **10b** at 1, 2.5, 5  $\mu\text{M}$ , respectively (Fig. 5a). While the results revealed that sophoridine could induce G1 cell cycle arrest (Fig. 5b). Combining the results of cell cycle assay and molecular docking analysis, we hypothesized that the difference between cell cycle arrest mechanisms of **10b** and sophoridine were caused by the binding modes. It is well recognized that the effects of Topo I inhibitors depend on two routes: catalyst inhibition and poison inhibition. The catalytic inhibitors can react with Topo I and suppress the enzymatic activity, causing the DNA duplication defeat. The poison inhibitors can bind to the covalent Topo I-DNA complex, consequently leading to double strand breaks and ultimately apoptotic cell death [38]. Due to the binding model of **10b** (Fig. 4) similar with camptothecin (Figs. 2a), **10b** can serve as poison inhibitor and induced S cell cycle arrest. While sophoridine serve as a catalytic inhibitor, which induced G1 cell cycle arrest.

### 3.7. *In vivo* antitumor activity of **10b** against HepG2 cells

Tumor xenografts derived from HepG2 cells were used to evaluate the antitumor effect of compound **10b** *in vivo*. Compared

with vehicle control and sophoridine group, the tumor growth of compound **10b** group was significantly inhibited (**10b** vs vehicle:  $p = 0.003$ ; **10b** vs sophoridine:  $p = 0.002$ , at day 25) (Fig. 6A, B). The value of T/C in the 40 mg/kg **10b** group and sophoridine group was 55.99% and 93.38%, respectively (day 25, volume of vehicle control =  $1185.78 \pm 137.44 \text{ mm}^3$ , volume of sophoridine group =  $1204.27 \pm 141.01 \text{ mm}^3$ , volume of **10b** group =  $737.04 \pm 109.29 \text{ mm}^3$ ). There was also a significant tumor weight loss in **10b** group compared with vehicle control ( $p = 0.039$ ) and sophoridine group ( $p = 0.005$ ). The tumor weight for each group was  $0.84 \pm 0.09 \text{ g}$  (vehicle),  $0.97 \pm 0.09 \text{ g}$  (sophoridine) and  $0.61 \pm 0.15 \text{ g}$  (**10b**) (Fig. 6C). In the 40 mg/kg irinotecan group, the value of T/C and tumor weight was 35.08% and  $0.47 \pm 0.12 \text{ g}$  (day 25). Although irinotecan displayed more potent antitumor activity than **10b**, irinotecan also exhibited more toxicity than **10b**, reflected by mouse body weight loss from day 19 (Fig. 6D).

## 4. Conclusion

Novel Topo I inhibitors were synthesized and tested for their cytotoxic activities. Further studies verified the consistency between docking and activity (antiproliferative activity and Topo I inhibitory activities) and the rationality of the design strategy. The SAR analysis and molecular model revealed that (i) the stacking force caused by indole moiety with base pairs is the primary affinity and its extent was dependent on the electron cloud; (ii) introduction of an aryl or alkyl group on the nitrogen atom of the indole enhanced the activity via improving the lipophilicity. Among the analogues, **10b** was chosen as a representative for further study due to its potent inhibitory potency against Topo I and antiproliferative activity against HepG2 cells. Compound **10b** arrested HepG2 cells at the S phase in a dose-dependent manner. The *in vivo* studies further demonstrated that **10b** significantly suppressed the growth of HepG2 xenograft tumors without adverse toxicity as no distinct weight loss of mice was observed. Taken together, the sophoridine scaffold of novel Topo I inhibitors could serve not only as a “carrier” to transport the indole moiety to the target, but it can also render many pharmacological advantages to the new inhibitors. Furthermore, the indole moiety significantly enhanced the biological activities. The new strategy provided a series novel Topo I inhibitors for further optimization and development in cancer therapy.

## 5. Experimental

### 5.1. Molecular docking and molecular modeling

Glide model from Schrödinger software was used for the molecular docking studies. The structure of the compounds was sketched using ChemDraw and optimized to lower energy conformers using Ligprep (Schrodinger LLC, New York, NY, USA). The structure of human DNA-Topo I complex (PDB ID: 1T8I) was downloaded from the Protein Data Bank and protein preparation wizard was used to prepare complex for docking. OPLS3 force field was used for optimizing the hydrogen bond network in the enzyme structure after a series of preprocessing, such as mutation, adding hydrogens, deleting water etc. 0.30 Å was a maximum cutoff of the energy converged or the route mean square deviation (RMSD). The receptor grid can be set up and generated from the Receptor Grid Generation panel. Ultimately, the generated grid of protein structure was used to perform docking with the compounds using Ligand Docking under the XP (extra precision) precision. Glide (docking) score is the evaluation standard of ligand-protein binding.

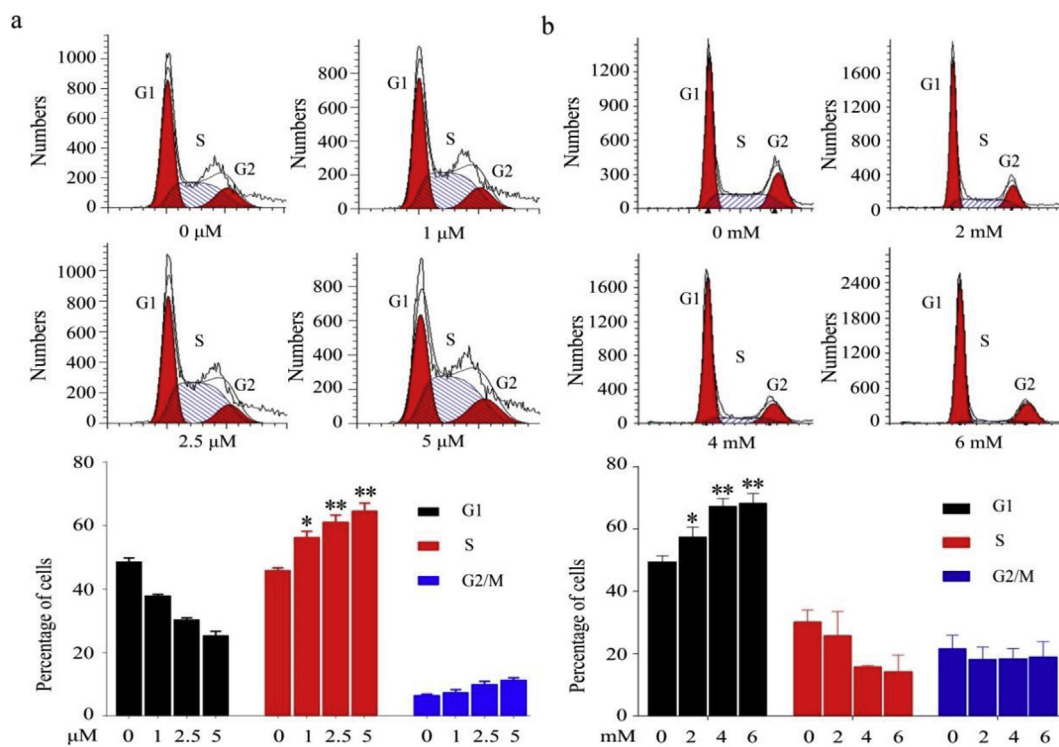


**Fig. 5.** Cell cycle analysis of compound **10b** and sophoridine. HepG2 cells were incubated without (control) or with **10b** at different concentrations (1, 2.5, 5 μM) (a) or with sophoridine at different concentrations (2, 4, 6 mM) (b) for 24 h and then analyzed for their cell cycle distribution using flow cytometry. The percentage of each population was shown as mean ± SD. Data is the representative of three independent experiments. \* $p < 0.05$ , \*\* $p < 0.01$ .

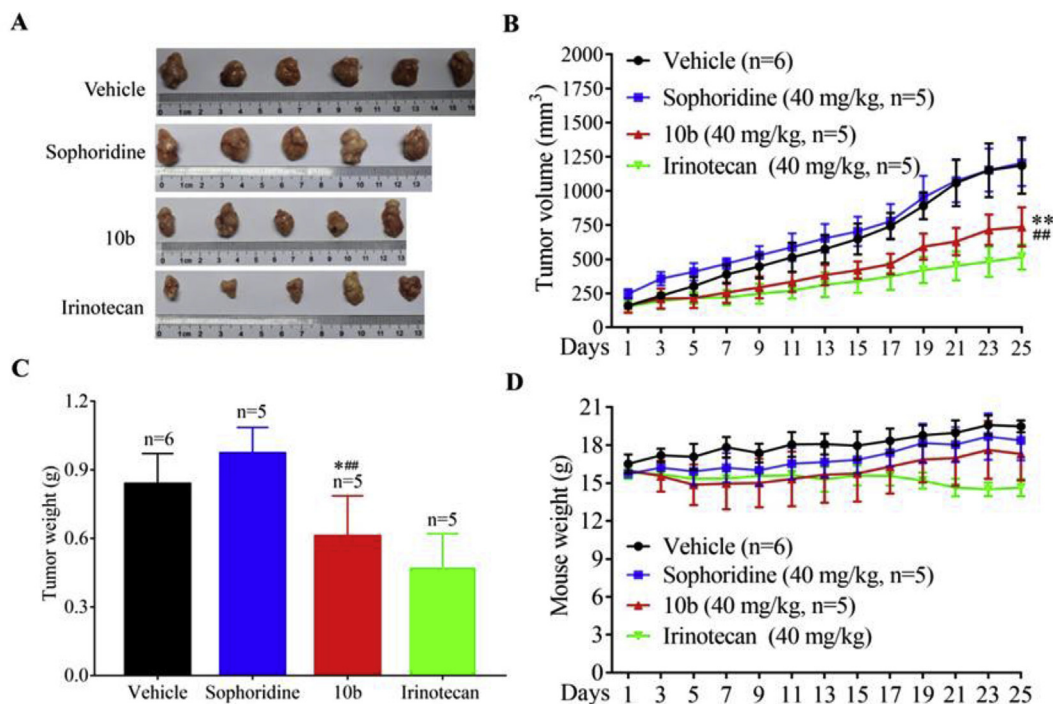


**Fig. 6.** *In vivo* antitumor activity of **10b** against liver cancer model in mice. (A) Image of the internal tumor tissues after anatomy; (B) Relationship curves of tumor volumes at various times (1d, 3d, 5d, 7d, 9d, 11d, 13d, 15d, 17d, 19d, 21d, 23d and 25d) after administration; (C) Average mass of internal tumor tissues of mice; (D) Relationship curves of mice body weights at various times (1d, 3d, 5d, 7d, 9d, 11d, 13d, 15d, 17d, 19d, 21d, 23d and 25d) after administration; Data expressed as the mean ± SD; statistical significance: compared with vehicle by *t*-test, \* $p < 0.05$ , \*\* $p < 0.01$ ; compared with sophoridine by *t*-test, # $p < 0.05$ , ## $p < 0.01$ .

## 5.2. Chemistry

All the chemicals were purchased from commercial sources and used without further purification unless otherwise stated. All the compounds were characterized by  $^1\text{H}$  NMR,  $^{13}\text{C}$  NMR and ESI-MS spectral analyses. Bruker Avance 600 (600 MHz) spectrometer was used for recording  $^1\text{H}$  and  $^{13}\text{C}$  nuclear magnetic resonance (NMR) data using  $\text{CDCl}_3$  as solvent and TMS as an internal standard. Chemical shifts are reported in  $\delta$  ppm relative to internal tetramethylsilane standard (TMS,  $\delta$  0.00). Coupling constants (J) were in hertz (Hz) and the peak patterns are indicated as follows: s, singlet; d, doublet; t, triplet; m, multiplet; q, quartet; br, broad, etc. The progress of reactions was monitored by thin-layer chromatography (TLC). Detections were done by UV light (254 nm) illumination and/or treatment with Bismuth potassium iodide solution. The products were purified by flash column chromatography equipped with commercial silica gel (300–400 mesh). Mass spectra were obtained from a ThermoFisher LCQ Fleet (ESI). Melting points were determined in open capillary tubes on X-4 melting point apparatus without correction.

### 5.2.1. General procedure for compound **3**

Sophoridine **1** (2.48g, 10 mmol) was hydrolyzed with 50 mL of aqueous NaOH (2 mol/L) under reflux for 8 h, and then solvent was evaporated to get **2** in crude form.  $\text{SOCl}_2$  (3 mL) was added to methanol (40 mL) and stirred for 30 min in ice-bath. Product **2** was then added portion-wise and the mixture was then refluxed for 3 h. After completion of the reaction, the mixture was filtered and solvent was concentrated to obtain **3**.

### 5.2.2. General procedure for compound **4a–4k**

A 50 mL flask was charged with **3** (1 mmol), acetic acid (1.5 mmol), formaldehyde (1.1 mmol, 36% aq) and  $\text{R}_1$  bearing indole and  $\text{H}_2\text{O}$  or  $\text{CH}_2\text{Cl}_2$  (3 mL). The reaction mixture was stirred at room temperature and progress of the reaction was monitored by TLC. After completion of the reaction, the mixture was poured into 10 mL of water and its pH was adjusted to 11–13 by diluted NaOH (20% aq.). The mixture was then extracted with  $\text{CH}_2\text{Cl}_2$  ( $3 \times 10$  mL), the combined organic layers were dried over anhydrous  $\text{MgSO}_4$  for 12 h and filtered. The solvent was evaporated under reduced pressure to give the crude product, which was purified by column chromatography using silica gel (300–400 mesh), eluted with a mixture of  $\text{CH}_2\text{Cl}_2$  and MeOH (5:1–3:1).

**5.2.2.1. Methyl 12-N-3-indolosophoridininate dihydrochloride (4a).** White solid; Yield: 91%; Mp: 154–156 °C;  $^1\text{H}$  NMR (600 MHz, Chloroform-*d*)  $\delta$  8.34 (s, 1H), 7.79–7.73 (m, 1H), 7.36 (d,  $J = 8.1$  Hz, 1H), 7.20 (m, 1H), 7.12 (m, 1H), 7.07 (d,  $J = 2.2$  Hz, 1H), 3.78–3.71 (m, 2H), 3.69 (s, 3H), 3.05–2.91 (m, 3H), 2.83 (m, 1H), 2.68 (d,  $J = 8.4$  Hz, 1H), 2.56–2.45 (m, 2H), 2.33 (m, 2H), 2.12–1.98 (m, 3H), 1.88–1.60 (m, 6H), 1.50 (m, 3H), 1.39–1.31 (m, 1H), 1.29–1.22 (m, 1H), 1.12–1.01 (m, 1H).  $^{13}\text{C}$  NMR (151 MHz,  $\text{CDCl}_3$ )  $\delta$  174.09, 136.71, 127.69, 122.97, 121.86, 120.16, 119.07, 114.58, 110.99, 63.68, 59.26, 54.53, 51.53, 51.37, 50.52, 45.49, 38.30, 34.31, 29.66, 27.09, 25.95, 25.32, 23.35, 22.18, 19.18. HR-MS (ESI)  $m/z$ : calculated for  $\text{C}_{25}\text{H}_{35}\text{N}_3\text{O}_2$   $[\text{M}+\text{H}]^+$ : MS: 410.2802, found: 410.2806.

**5.2.2.2. Methyl 12-N-3-(5-methyl)indolosophoridininate dihydrochloride (4b).** Green solid; Yield: 83%; Mp: 62–64 °C;  $^1\text{H}$  NMR (600 MHz, Chloroform-*d*)  $\delta$  8.10 (s, 1H), 7.57–7.53 (m, 1H), 7.25 (d,  $J = 8.2$  Hz, 1H), 7.03 (m, 2H), 3.75–3.71 (m, 2H), 3.69 (s, 3H), 3.04–2.89 (m, 3H), 2.80 (m, 1H), 2.68 (d,  $J = 8.6$  Hz, 1H), 2.53–2.43 (m, 5H), 2.33 (t,  $J = 6.8$  Hz, 2H), 2.15–1.98 (m, 3H), 1.78 (m, 3H), 1.66 (m, 3H), 1.57–1.46 (m, 3H), 1.37 (m, 1H), 1.25–1.19 (m, 1H), 1.11–1.02 (m, 1H).  $^{13}\text{C}$  NMR (151 MHz,  $\text{CDCl}_3$ )  $\delta$  174.07, 134.97, 128.21, 127.94,

123.44, 123.00, 119.84, 114.25, 110.56, 63.74, 59.21, 54.73, 51.50, 51.47, 50.54, 45.56, 38.56, 34.37, 29.91, 26.92, 26.32, 25.49, 23.40, 22.30, 21.54, 19.27. HR-MS (ESI)  $m/z$ : calculated for  $\text{C}_{26}\text{H}_{37}\text{N}_3\text{O}_2$   $[\text{M}+\text{H}]^+$ : 424.2959, found: 424.2957.

**5.2.2.3. Methyl 12-N-3-(5-methoxy)indolosophoridininate dihydrochloride (4c).** Brown solid; Yield: 85%; Mp: 116–118 °C;  $^1\text{H}$  NMR (600 MHz, Chloroform-*d*)  $\delta$  8.20 (s, 1H), 7.26–7.22 (m, 2H), 7.04 (d,  $J = 2.2$  Hz, 1H), 6.86 (m, 1H), 3.88 (s, 3H), 3.75–3.70 (m, 2H), 3.69 (s, 3H), 3.06–2.92 (m, 3H), 2.91–2.85 (m, 1H), 2.69 (d,  $J = 8.0$  Hz, 1H), 2.60–2.46 (m, 2H), 2.38–2.29 (m, 2H), 2.12–1.98 (m, 3H), 1.89 (m, 1H), 1.78–1.61 (m, 5H), 1.57–1.45 (m, 3H), 1.39 (m, 1H), 1.31–1.23 (m, 1H), 1.11–1.02 (m, 1H).  $^{13}\text{C}$  NMR (151 MHz,  $\text{CDCl}_3$ )  $\delta$  174.08, 153.61, 131.84, 128.05, 123.70, 114.23, 112.29, 111.68, 101.89, 63.81, 59.22, 55.79, 54.28, 51.53, 51.03, 50.70, 45.39, 38.07, 34.28, 29.43, 27.20, 25.63, 25.33, 23.31, 22.16, 19.10. HR-MS (ESI)  $m/z$ : calculated for  $\text{C}_{26}\text{H}_{37}\text{N}_3\text{O}_3$   $[\text{M}+\text{H}]^+$ : 440.2908, found: 440.2913.

**5.2.2.4. Methyl 12-N-3-(5-cyan)indolosophoridininate dihydrochloride (4d).** Brown oil; Yield: 93%;  $^1\text{H}$  NMR (600 MHz, Chloroform-*d*)  $\delta$  9.46 (s, 1H), 8.11 (d,  $J = 1.5$  Hz, 1H), 7.46–7.38 (m, 2H), 7.21 (s, 1H), 3.78–3.71 (m, 2H), 3.68 (s, 3H), 3.23–3.04 (m, 3H), 3.03–2.94 (m, 1H), 2.83–2.73 (m, 1H), 2.56 (m, 2H), 2.37–2.21 (m, 2H), 2.20–2.10 (m, 2H), 2.07–1.17 (m, 11H), 1.12 (m, 1H), 0.94–0.81 (m, 1H).  $^{13}\text{C}$  NMR (151 MHz,  $\text{CDCl}_3$ )  $\delta$  174.00, 138.56, 127.36, 125.88, 125.38, 124.79, 121.07, 114.73, 112.13, 101.97, 62.71, 58.79, 52.93, 51.56, 51.44, 49.92, 44.95, 36.83, 34.00, 29.69, 27.93, 24.17, 23.79, 23.09, 21.68, 18.73. HR-MS (ESI)  $m/z$ : calculated for  $\text{C}_{26}\text{H}_{34}\text{N}_4\text{O}_2$   $[\text{M}+\text{H}]^+$ : 435.2755, found: 435.2756.

**5.2.2.5. Methyl 12-N-3-(5-nitro)indolosophoridininate dihydrochloride (4e).** Green oil; Yield: 87%;  $^1\text{H}$  NMR (600 MHz, Chloroform-*d*)  $\delta$  8.59 (d,  $J = 2.2$  Hz, 1H), 8.12 (m, 1H), 7.43 (d,  $J = 9.0$  Hz, 1H), 7.32 (d,  $J = 3.3$  Hz, 1H), 6.69 (d,  $J = 3.2$  Hz, 1H), 4.86 (m, 2H), 3.71 (s, 3H), 3.46–3.29 (m, 2H), 3.25–3.10 (m, 2H), 3.06 (m, 1H), 2.79 (m, 1H), 2.55 (m, 2H), 2.45 (m, 2H), 2.39–2.21 (m, 2H), 2.13 (m, 1H), 1.94–1.46 (m, 8H), 1.38–1.14 (m, 3H).  $^{13}\text{C}$  NMR (151 MHz,  $\text{CDCl}_3$ )  $\delta$  173.77, 141.96, 138.93, 131.05, 128.45, 118.21, 117.38, 110.21, 104.27, 66.45, 62.30, 59.61, 52.86, 51.68, 48.58, 45.28, 35.56, 33.45, 28.36, 26.88, 23.97, 23.08, 22.59, 22.53, 18.25. HR-MS (ESI)  $m/z$ : calculated for  $\text{C}_{25}\text{H}_{34}\text{N}_4\text{O}_4$   $[\text{M}+\text{H}]^+$ : 455.2653, found: 455.2657.

**5.2.2.6. Methyl 12-N-3-(5-chloro)indolosophoridininate dihydrochloride (4f).** Brown oil; Yield: 92%;  $^1\text{H}$  NMR (600 MHz, Chloroform-*d*)  $\delta$  8.27 (s, 1H), 7.69 (d,  $J = 2.1$  Hz, 1H), 7.31 (d,  $J = 8.6$  Hz, 1H), 7.16 (m, 1H), 7.12 (s, 1H), 3.76–3.71 (m, 2H), 3.70 (s, 3H), 3.38–3.15 (m, 3H), 3.10 (d,  $J = 13.5$  Hz, 1H), 3.00 (d,  $J = 11.7$  Hz, 1H), 2.74–2.56 (m, 2H), 2.44–2.26 (m, 2H), 2.27–2.12 (m, 3H), 2.09–1.23 (m, 10H), 1.17 (m, 1H), 0.93–0.83 (m, 1H).  $^{13}\text{C}$  NMR (151 MHz,  $\text{CDCl}_3$ )  $\delta$  173.96, 135.08, 128.55, 124.89, 124.73, 122.32, 119.42, 113.17, 112.29, 62.53, 60.20, 52.98, 51.59, 50.54, 49.95, 45.39, 36.01, 33.87, 28.62, 27.16, 23.22, 22.91, 22.87, 21.70, 18.44. HR-MS (ESI)  $m/z$ : calculated for  $\text{C}_{25}\text{H}_{34}\text{ClN}_3\text{O}_2$   $[\text{M}+\text{H}]^+$ : 444.2412, found: 444.2415.

**5.2.2.7. Methyl 12-N-3-(5-bromo)indolosophoridininate dihydrochloride (4g).** White solid; Yield: 89%; Mp: 58–60 °C;  $^1\text{H}$  NMR (600 MHz, Chloroform-*d*)  $\delta$  9.06–8.87 (m, 1H), 7.92 (t,  $J = 2.1$  Hz, 1H), 7.24 (m, 1H), 7.21–7.15 (m, 1H), 7.05 (d,  $J = 2.5$  Hz, 1H), 3.68 (m, 5H), 3.04–2.89 (m, 3H), 2.79 (m, 1H), 2.64–2.58 (m, 1H), 2.53–2.39 (m, 2H), 2.29 (m, 2H), 2.14–1.94 (m, 3H), 1.84–1.68 (m, 3H), 1.68–1.38 (m, 6H), 1.33 (d,  $J = 13.6$  Hz, 1H), 1.24–1.17 (m, 1H), 1.10–1.01 (m, 1H).  $^{13}\text{C}$  NMR (151 MHz,  $\text{CDCl}_3$ )  $\delta$  174.04, 135.36, 129.47, 124.52, 124.24, 122.91, 114.20, 112.47, 112.19, 63.43, 59.14, 54.69, 51.68, 51.54, 50.36, 45.56, 38.55, 34.28, 29.90, 26.92, 26.31, 25.50, 23.33, 22.17, 19.25. HR-MS (ESI)  $m/z$ : calculated for

$C_{25}H_{34}BrN_3O_2$   $[M+H]^+$ : 488.1907, found: 488.1911.

**5.2.2.8. Methyl 12-N-3-(5-fluoro)indolosporidinate dihydrochloride (4h).** Brown solid; Yield: 88%; Mp: 136–138 °C;  $^1H$  NMR (600 MHz, Chloroform-*d*)  $\delta$  8.23 (s, 1H), 7.42 (m, 1H), 7.26 (m, 1H), 7.11 (d,  $J = 2.2$  Hz, 1H), 6.95 (m, 1H), 3.70 (d,  $J = 2.4$  Hz, 2H), 3.69 (s, 3H), 3.03–2.94 (m, 3H), 2.81 (m, 1H), 2.62 (d,  $J = 8.5$  Hz, 1H), 2.53–2.43 (m, 2H), 2.32 (m, 2H), 2.13–1.97 (m, 3H), 1.83–1.75 (m, 3H), 1.69–1.42 (m, 6H), 1.36–1.27 (m, 1H), 1.26–1.20 (m, 1H), 1.12–1.00 (m, 1H).  $^{13}C$  NMR (151 MHz,  $CDCl_3$ )  $\delta$  174.05, 157.51 (d,  $J = 233.8$  Hz), 133.17, 128.10, 124.63, 114.87, 111.44, 110.28, 105.11, 63.46, 59.15, 54.63, 51.65, 51.52, 50.43, 45.52, 38.44, 34.30, 29.85, 27.00, 26.17, 25.47, 23.36, 22.09, 19.23. HR-MS (ESI)  $m/z$ : calculated for  $C_{25}H_{34}FN_3O_2$   $[M+Na]^+$ : 450.2527, found: 450.2533.

**5.2.2.9. Methyl 12-N-3-(4-fluoro)indolosporidinate dihydrochloride (4i).** Yellow oil; Yield: 89%;  $^1H$  NMR (600 MHz, Chloroform-*d*)  $\delta$  8.99 (s, 1H), 7.12–7.03 (m, 3H), 6.77–6.69 (m, 1H), 3.87–3.71 (m, 2H), 3.67 (s, 3H), 3.01–2.90 (m, 3H), 2.80 (m, 1H), 2.70 (d,  $J = 9.5$  Hz, 1H), 2.55–2.46 (m, 2H), 2.32 (t,  $J = 6.9$  Hz, 2H), 2.14–1.95 (m, 3H), 1.76 (m, 3H), 1.70–1.45 (m, 6H), 1.36–1.29 (m, 1H), 1.24–1.18 (m, 1H), 1.11–1.02 (m, 1H).  $^{13}C$  NMR (151 MHz,  $CDCl_3$ )  $\delta$  174.11, 157.32 (d,  $J = 247.7$  Hz), 139.44, 123.14, 122.07, 116.24, 113.72, 107.16, 104.40, 64.00, 59.17, 54.71, 51.49, 51.42, 50.70, 45.51, 38.52, 34.31, 29.92, 26.95, 26.26, 25.31, 23.42, 22.87, 19.28. HR-MS (ESI)  $m/z$ : calculated for  $C_{25}H_{34}FN_3O_2$   $[M+H]^+$ : 428.2708, found: 428.2709.

**5.2.2.10. Methyl 12-N-3-(6-fluoro)indolosporidinate dihydrochloride (4j).** Brown oil; Yield: 87%;  $^1H$  NMR (600 MHz, Chloroform-*d*)  $\delta$  8.66 (s, 1H), 7.67 (m, 1H), 7.07–6.98 (m, 2H), 6.90–6.81 (m, 1H), 3.70 (d,  $J = 2.3$  Hz, 2H), 3.68 (s, 3H), 3.00–2.92 (m, 3H), 2.78 (m, 1H), 2.61 (d,  $J = 9.6$  Hz, 1H), 2.49–2.42 (m, 2H), 2.30 (t,  $J = 6.2$  Hz, 2H), 2.10–1.92 (m, 3H), 1.79–1.73 (m, 3H), 1.63 (m, 3H), 1.56–1.41 (m, 3H), 1.29–1.26 (m, 1H), 1.24–1.17 (m, 1H), 1.10–0.97 (m, 1H).  $^{13}C$  NMR (151 MHz,  $CDCl_3$ )  $\delta$  174.08, 159.90 (d,  $J = 236.8$  Hz), 136.62, 124.25, 123.22, 120.88, 114.61, 107.69, 97.27, 63.55, 59.14, 54.68, 51.61, 51.51, 50.49, 45.51, 38.50, 34.28, 29.90, 26.95, 26.25, 25.53, 23.35, 22.13, 19.24. HR-MS (ESI)  $m/z$ : calculated for  $C_{25}H_{34}FN_3O_2$   $[M+H]^+$ : 428.2708, found: 428.2711.

**5.2.2.11. Methyl 12-N-3-(2-methyl formate)indolosporidinate dihydrochloride (4k).** Yellow solid; Yield: 67%; Mp: 104–106 °C;  $^1H$  NMR (600 MHz, Chloroform-*d*)  $\delta$  8.86 (s, 1H), 7.92 (d,  $J = 8.1$  Hz, 1H), 7.41–7.36 (m, 1H), 7.34 (m, 1H), 7.15 (m, 1H), 4.43 (m, 2H), 4.24–3.97 (m, 2H), 3.69 (s, 3H), 2.94 (m, 4H), 2.68 (d,  $J = 9.5$  Hz, 1H), 2.54 (d,  $J = 11.2$  Hz, 1H), 2.42 (m, 1H), 2.34 (t,  $J = 7.2$  Hz, 2H), 2.13 (t,  $J = 11.2$  Hz, 1H), 2.08–1.91 (m, 2H), 1.86 (m, 1H), 1.77–1.47 (m, 8H), 1.45 (t,  $J = 7.1$  Hz, 3H), 1.34–1.23 (m, 2H), 1.07 (m, 1H).  $^{13}C$  NMR (151 MHz,  $CDCl_3$ )  $\delta$  173.97, 162.30, 135.89, 128.55, 125.51, 124.19, 122.61, 122.13, 119.99, 111.53, 64.65, 60.84, 58.88, 54.24, 51.49, 51.25, 48.84, 45.33, 38.13, 34.38, 29.53, 27.13, 25.76, 25.25, 23.50, 22.60, 19.11, 14.47. HR-MS (ESI)  $m/z$ : calculated for  $C_{27}H_{37}N_3O_4$   $[M+H]^+$ : 468.2857, found: 468.2861.

### 5.2.3. General procedure for compound 5a-5p

NaH (216 mg, 5.40 mmol, 1.08 eq) was added portion wise to a solution of  $R_1$  bearing indole (5.00 mmol, 1.0 eq.) in DMF (20 mL) at 0 °C. The ice bath was removed and the mixture was stirred for 30 min. Halides (5.25 mmol, 1.05 eq.) were then added dropwise at 0 °C and the reaction mixture was stirred at room temperature. The progress of the reaction was monitored by TLC. After the completion of the reaction, addition of  $H_2O$  (10 mL) was followed by extraction with EtOAc (3  $\times$  20 mL). The combined organic layers were washed with brine and then dried over  $MgSO_4$ . All volatiles

were removed in vacuo to obtain desired **5a-5p** without purification.

### 5.2.4. General procedure for compound 6a-6p

A 50 mL flask was charged with **3** (1 mmol), acetic acid (1.5 mmol), formaldehyde (1.1 mmol, 36% aq), **5a-5p** and  $H_2O$  or  $CH_2Cl_2$  (3 mL). The reaction mixture was stirred at room temperature. The progress of the reaction was monitored by TLC. After completion of the reaction, the mixture was poured into 10 mL water and its pH was adjusted to 11–13 by diluted NaOH (20% aq.). The mixture was extracted with  $CH_2Cl_2$  (3  $\times$  10 mL) and the combined organic layers were dried over anhydrous  $MgSO_4$  for 12 h followed by filtration. The solvent was evaporated under reduced pressure to give the crude product, which was purified by column chromatography using silica gel (300–400 mesh), eluted with a mixture of  $CH_2Cl_2$  and MeOH (5:1–3:1).

**5.2.4.1. Methyl 12-N-3-(N-methyl)indolosporidinate dihydrochloride (6a).** Yellow oil; Yield: 86%;  $^1H$  NMR (600 MHz, Chloroform-*d*)  $\delta$  7.77 (m, 1H), 7.29 (d,  $J = 8.0$  Hz, 1H), 7.24 (m, 1H), 7.12 (m, 1H), 6.92 (s, 1H), 3.75 (s, 3H), 3.75–3.72 (m, 2H), 3.70 (s, 3H), 3.04–2.91 (m, 3H), 2.80 (m, 1H), 2.69 (m, 1H), 2.49 (m, 2H), 2.37–2.32 (m, 2H), 2.13–1.98 (m, 3H), 1.84–1.60 (m, 6H), 1.52 (m, 3H), 1.38–1.32 (m, 1H), 1.24–1.18 (m, 1H), 1.07 (m, 1H).  $^{13}C$  NMR (151 MHz,  $CDCl_3$ )  $\delta$  174.01, 137.40, 128.15, 127.61, 121.47, 120.25, 118.61, 113.23, 109.01, 63.85, 59.23, 54.74, 51.49, 51.39, 50.47, 45.56, 38.53, 34.37, 32.61, 29.91, 26.95, 26.29, 25.54, 23.41, 22.25, 19.28. HR-MS (ESI)  $m/z$ : calculated for  $C_{26}H_{37}N_3O_2$   $[M+Na]^+$ : 422.2778, found: 422.2783.

**5.2.4.2. Methyl 12-N-3-(N-ethyl)indolosporidinate dihydrochloride (6b).** Yellow oil; Yield: 84%;  $^1H$  NMR (600 MHz, Chloroform-*d*)  $\delta$  7.69–7.66 (m, 1H), 7.33 (d,  $J = 8.2$  Hz, 1H), 7.23–7.19 (m, 1H), 7.11–7.07 (m, 1H), 7.00 (s, 1H), 4.14 (q,  $J = 7.3$  Hz, 2H), 3.78–3.71 (m, 2H), 3.69 (s, 3H), 3.37–3.27 (m, 2H), 3.19 (m, 1H), 3.13 (m, 1H), 3.04–2.97 (m, 1H), 2.77–2.71 (m, 1H), 2.65 (d,  $J = 7.4$  Hz, 1H), 2.44–2.28 (m, 3H), 2.25–2.05 (m, 4H), 1.89 (m, 1H), 1.79–1.58 (m, 5H), 1.55–1.41 (m, 6H), 1.16 (m, 1H).  $^{13}C$  NMR (151 MHz,  $CDCl_3$ )  $\delta$  173.92, 136.48, 128.07, 126.30, 121.52, 120.02, 118.73, 112.04, 109.32, 62.99, 60.21, 54.81, 52.98, 51.55, 50.17, 45.31, 40.79, 36.06, 33.98, 28.59, 27.18, 23.27, 22.95, 22.89, 21.85, 18.46, 15.47. HR-MS (ESI)  $m/z$ : calculated for  $C_{27}H_{39}N_3O_2$   $[M+H]^+$ : 438.3115, found: 438.3117.

**5.2.4.3. Methyl 12-N-3-(N-butyl)indolosporidinate dihydrochloride (6c).** Yellow oil; Yield: 85%;  $^1H$  NMR (600 MHz, Chloroform-*d*)  $\delta$  7.66 (m, 1H), 7.28 (d,  $J = 8.1$  Hz, 1H), 7.16 (m, 1H), 7.05 (m, 1H), 6.94 (s, 1H), 4.04 (t,  $J = 7.1$  Hz, 2H), 3.74–3.66 (m, 2H), 3.64 (s, 3H), 3.20–3.00 (m, 4H), 2.85–2.77 (m, 1H), 2.67 (q,  $J = 3.0$  Hz, 1H), 2.55 (d,  $J = 7.2$  Hz, 1H), 2.31 (m, 2H), 2.19–1.91 (m, 5H), 1.83–1.58 (m, 6H), 1.58–1.33 (m, 5H), 1.33–1.23 (m, 2H), 1.15–1.03 (m, 1H), 0.90 (t,  $J = 7.4$  Hz, 3H).  $^{13}C$  NMR (151 MHz,  $CDCl_3$ )  $\delta$  173.88, 136.69, 128.04, 126.96, 121.38, 120.05, 118.58, 112.12, 109.35, 62.97, 59.88, 53.48, 51.48, 50.67, 50.16, 45.86, 45.34, 36.75, 34.06, 32.27, 28.03, 27.98, 23.93, 23.91, 23.05, 21.87, 20.14, 18.66, 13.69. HR-MS (ESI)  $m/z$ : calculated for  $C_{29}H_{43}N_3O_2$   $[M+H]^+$ : 466.3428, found: 466.3429.

**5.2.4.4. Methyl 12-N-3-(N-cyclopropyl)indolosporidinate dihydrochloride (6d).** Green oil; Yield: 87%;  $^1H$  NMR (600 MHz, Chloroform-*d*)  $\delta$  7.78 (d,  $J = 7.9$  Hz, 1H), 7.31 (d,  $J = 8.2$  Hz, 1H), 7.20 (m, 1H), 7.12–7.09 (m, 1H), 7.08 (s, 1H), 3.96–3.87 (m, 2H), 3.79–3.72 (m, 2H), 3.67 (s, 3H), 3.02–2.91 (m, 3H), 2.79 (m, 1H), 2.66 (d,  $J = 8.9$  Hz, 1H), 2.48 (m, 2H), 2.32 (t,  $J = 6.8$  Hz, 2H), 2.14–1.99 (m, 3H), 1.78 (m, 3H), 1.66 (m, 3H), 1.58–1.44 (m, 3H), 1.36–1.30 (m, 1H), 1.29–1.16 (m, 2H), 1.07 (m, 1H), 0.65–0.55 (m,

2H), 0.35 (m, 2H).  $^{13}\text{C}$  NMR (151 MHz,  $\text{CDCl}_3$ )  $\delta$  173.93, 136.86, 128.23, 126.38, 121.35, 120.32, 118.59, 113.04, 109.20, 63.32, 59.23, 54.78, 51.77, 51.43, 50.52, 50.35, 45.56, 38.54, 34.32, 30.02, 26.94, 26.38, 25.57, 23.40, 22.11, 19.33, 11.36, 4.08, 4.04. HR-MS (ESI)  $m/z$ : calculated for  $\text{C}_{29}\text{H}_{41}\text{N}_3\text{O}_2$   $[\text{M}+\text{H}]^+$ : 464.3272, found: 464.3277.

**5.2.4.5. Methyl 12-N-3-(N-benzyl)indolosporidinolate dihydrochloride (6e).** Yellow oil; Yield: 82%;  $^1\text{H}$  NMR (600 MHz, Chloroform-*d*)  $\delta$  7.78 (m, 1H), 7.33–7.29 (m, 2H), 7.28–7.24 (m, 2H), 7.19 (m, 1H), 7.14–7.09 (m, 3H), 7.01 (s, 1H), 5.30 (s, 2H), 3.79–3.72 (m, 2H), 3.68 (s, 3H), 3.06–2.93 (m, 3H), 2.89 (m, 1H), 2.68 (d,  $J = 8.9$  Hz, 1H), 2.59–2.48 (m, 2H), 2.37–2.26 (m, 2H), 2.10–1.95 (m, 3H), 1.88–1.60 (m, 6H), 1.59–1.41 (m, 3H), 1.38–1.23 (m, 2H), 1.09 (m, 1H).  $^{13}\text{C}$  NMR (151 MHz,  $\text{CDCl}_3$ )  $\delta$  174.00, 137.74, 137.07, 128.71 (2), 128.36, 127.52, 127.07, 126.77 (2), 121.71, 120.36, 118.91, 113.78, 109.51, 63.55, 59.10, 54.28, 51.49, 51.43, 50.42, 49.88, 45.37, 38.13, 34.31, 29.56, 27.19, 25.77, 25.22, 23.36, 22.10, 19.16. HR-MS (ESI)  $m/z$ : calculated for  $\text{C}_{32}\text{H}_{41}\text{N}_3\text{O}_2$   $[\text{M}+\text{H}]^+$ : 500.3272, found: 500.3275.

**5.2.4.6. Methyl 12-N-3-(N-2-fluorobenzyl)indolosporidinolate dihydrochloride (6f).** Yellow oil; Yield: 78%;  $^1\text{H}$  NMR (600 MHz, Chloroform-*d*)  $\delta$  7.71 (d,  $J = 7.9$  Hz, 1H), 7.34 (d,  $J = 8.3$  Hz, 1H), 7.26 (m, 1H), 7.22 (m, 1H), 7.16–7.05 (m, 3H), 7.02 (m, 1H), 6.91 (m, 1H), 5.40–5.30 (m, 2H), 3.78 (s, 2H), 3.68 (s, 3H), 3.49–3.32 (m, 2H), 3.22 (m, 2H), 3.07 (d,  $J = 11.9$  Hz, 1H), 2.80–2.67 (m, 2H), 2.41 (m, 2H), 2.35–2.05 (m, 5H), 1.93 (d,  $J = 12.6$  Hz, 1H), 1.83–1.62 (m, 5H), 1.47 (d,  $J = 12.3$  Hz, 3H), 1.22 (s, 1H).  $^{13}\text{C}$  NMR (151 MHz,  $\text{CDCl}_3$ )  $\delta$  173.86, 160.35 (d,  $J = 246.6$  Hz), 136.95, 129.53, 129.01, 128.07, 124.55, 124.41, 124.39, 122.10, 119.97, 119.32, 115.58, 115.44, 109.65, 62.78, 54.91, 53.12, 51.56, 50.36, 49.98, 45.48, 43.72, 35.90, 33.83, 28.61, 26.94, 23.04, 22.82, 22.77, 21.86, 18.40. HR-MS (ESI)  $m/z$ : calculated for  $\text{C}_{32}\text{H}_{40}\text{FN}_3\text{O}_2$   $[\text{M}+\text{H}]^+$ : 518.3177, found: 518.3172.

**5.2.4.7. Methyl 12-N-3-(N-3-fluorobenzyl)indolosporidinolate dihydrochloride (6g).** Yellow oil; Yield: 76%;  $^1\text{H}$  NMR (600 MHz, Chloroform-*d*)  $\delta$  7.67 (d,  $J = 7.9$  Hz, 1H), 7.25–7.17 (m, 2H), 7.17–7.11 (m, 1H), 7.10–7.05 (m, 1H), 7.01 (s, 1H), 6.89 (m, 2H), 6.70 (m, 1H), 5.24 (s, 2H), 3.78–3.68 (m, 2H), 3.62 (s, 3H), 3.36–3.22 (m, 2H), 3.17 (m, 1H), 3.14–3.06 (m, 1H), 3.04–2.96 (m, 1H), 2.75–2.68 (m, 1H), 2.64 (d,  $J = 8.7$  Hz, 1H), 2.41–2.31 (m, 2H), 2.31–2.02 (m, 5H), 1.85 (m, 1H), 1.78–1.06 (m, 9H).  $^{13}\text{C}$  NMR (151 MHz,  $\text{CDCl}_3$ )  $\delta$  173.78, 163.01 (d,  $J = 246.7$  Hz), 140.27, 136.97, 130.31, 128.17, 122.28, 122.06, 120.08, 119.27, 114.56, 114.43, 113.68, 113.53, 109.61, 62.73, 60.17, 52.90, 51.50, 50.36, 49.94, 49.35, 45.29, 35.88, 33.87, 28.59, 27.03, 23.17, 22.86, 22.73, 21.81, 18.38. HR-MS (ESI)  $m/z$ : calculated for  $\text{C}_{32}\text{H}_{40}\text{FN}_3\text{O}_2$   $[\text{M}+\text{H}]^+$ : 518.3177, found: 518.3179.

**5.2.4.8. Methyl 12-N-3-(N-4-fluorobenzyl)indolosporidinolate dihydrochloride (6h).** Yellow oil; Yield: 73%;  $^1\text{H}$  NMR (600 MHz, Chloroform-*d*)  $\delta$  7.70 (m, 1H), 7.26 (m, 1H), 7.20 (m, 1H), 7.14–7.06 (m, 3H), 7.02–6.95 (m, 3H), 5.26 (s, 2H), 3.76 (s, 2H), 3.68 (s, 3H), 3.46–3.35 (m, 2H), 3.29–3.17 (m, 2H), 3.07 (d,  $J = 11.6$  Hz, 1H), 2.76–2.62 (m, 2H), 2.40 (m, 1H), 2.36–2.26 (m, 2H), 2.25–2.04 (m, 4H), 1.96–1.88 (m, 1H), 1.82–1.59 (m, 5H), 1.53–1.39 (m, 3H), 1.25–1.15 (m, 1H).  $^{13}\text{C}$  NMR (151 MHz,  $\text{CDCl}_3$ )  $\delta$  173.92, 162.21 (d,  $J = 246.0$  Hz), 136.99, 133.24, 128.50 (2), 128.20, 127.30, 122.03, 120.11, 119.22, 115.65 (2), 112.71, 109.66, 62.81, 54.87, 53.15, 51.54, 50.37, 50.02, 49.27, 45.48, 36.05, 33.88, 28.67, 26.97, 23.11, 22.90, 22.83, 21.74, 18.42. HR-MS (ESI)  $m/z$ : calculated for  $\text{C}_{32}\text{H}_{40}\text{FN}_3\text{O}_2$   $[\text{M}+\text{H}]^+$ : 518.3177, Found: 518.3181.

**5.2.4.9. Methyl 12-N-3-(N-4-chlorobenzyl)indolosporidinolate dihydrochloride (6i).** Yellow oil; Yield: 74%;  $^1\text{H}$  NMR (600 MHz, Chloroform-*d*)  $\delta$  7.78 (m, 1H), 7.28–7.23 (m, 2H), 7.23–7.16 (m, 2H), 7.12 (m, 1H), 7.06–7.01 (m, 2H), 6.98 (s, 1H), 5.25 (s, 2H), 3.79–3.71 (m,

2H), 3.68 (s, 3H), 3.07–2.93 (m, 3H), 2.86 (m, 1H), 2.70–2.64 (m, 1H), 2.53 (m, 2H), 2.35–2.28 (m, 2H), 2.16–1.96 (m, 3H), 1.89–1.60 (m, 6H), 1.59–1.40 (m, 3H), 1.36–1.25 (m, 2H), 1.13–1.03 (m, 1H).  $^{13}\text{C}$  NMR (151 MHz,  $\text{CDCl}_3$ )  $\delta$  173.95, 136.93, 136.26, 133.33, 128.87 (2), 128.42, 128.11 (2), 126.89, 121.88, 120.48, 119.09, 114.07, 109.40, 63.48, 59.26, 54.50, 51.55, 51.50, 50.39, 49.25, 45.50, 38.21, 34.28, 29.64, 27.16, 25.89, 25.29, 23.35, 22.11, 19.18. HR-MS (ESI)  $m/z$ : calculated for  $\text{C}_{32}\text{H}_{40}\text{ClN}_3\text{O}_2$   $[\text{M}+\text{H}]^+$ : 534.2882, found: 534.2885.

**5.2.4.10. Methyl 12-N-3-(N-4-bromobenzyl)indolosporidinolate dihydrochloride (6j).** White solid; Yield: 76%; Mp: 76–78 °C;  $^1\text{H}$  NMR (600 MHz, Chloroform-*d*)  $\delta$  7.75 (m, 1H), 7.43–7.39 (m, 2H), 7.23–7.16 (m, 2H), 7.12 (m, 1H), 6.97 (d,  $J = 8.4$  Hz, 3H), 5.23 (s, 2H), 3.79–3.70 (m, 2H), 3.68 (s, 3H), 3.10 (m, 3H), 2.99 (m, 1H), 2.73 (m, 1H), 2.71–2.66 (m, 1H), 2.55 (d,  $J = 7.2$  Hz, 1H), 2.40–2.26 (m, 2H), 2.16–2.01 (m, 4H), 1.93–1.54 (m, 5H), 1.53–1.41 (m, 3H), 1.41–1.21 (m, 2H), 1.18–1.05 (m, 1H).  $^{13}\text{C}$  NMR (151 MHz,  $\text{CDCl}_3$ )  $\delta$  173.93, 136.95, 136.70, 131.84, 128.45, 128.34, 127.01, 121.95, 121.44, 120.37, 119.15, 113.71, 109.47, 63.25, 59.24, 53.53, 51.52, 51.11, 50.26, 49.32, 45.19, 37.23, 34.16, 28.66, 27.73, 24.58, 24.47, 23.21, 21.97, 18.88. HR-MS (ESI)  $m/z$ : calculated for  $\text{C}_{32}\text{H}_{40}\text{BrN}_3\text{O}_2$   $[\text{M}+\text{H}]^+$ : 578.2377, found: 578.2383.

**5.2.4.11. Methyl 12-N-3-(N-4-trifluoromethylbenzyl)indolosporidinolate dihydrochloride (6k).** Orange oil; Yield: 72%;  $^1\text{H}$  NMR (600 MHz, Chloroform-*d*)  $\delta$  7.80 (d,  $J = 7.8$  Hz, 1H), 7.56 (d,  $J = 8.0$  Hz, 2H), 7.24–7.17 (m, 4H), 7.14 (m, 1H), 7.01 (s, 1H), 5.35 (s, 2H), 3.81–3.72 (m, 2H), 3.68 (s, 3H), 3.05–2.91 (m, 3H), 2.83 (m, 1H), 2.67 (d,  $J = 8.8$  Hz, 1H), 2.54–2.46 (m, 2H), 2.32 (m, 2H), 2.15–1.96 (m, 3H), 1.86–1.60 (m, 6H), 1.59–1.43 (m, 3H), 1.34–1.24 (m, 2H), 1.14–1.02 (m, 1H).  $^{13}\text{C}$  NMR (151 MHz,  $\text{CDCl}_3$ )  $\delta$  173.96, 141.88, 136.93, 129.85 (q,  $J = 32.3$  Hz), 128.46, 126.92, 126.88 (2), 125.71 (2), 125.70, 122.00, 120.58, 119.21, 114.41, 109.31, 63.54, 59.21, 54.61, 51.66, 51.48, 50.39, 49.43, 45.51, 38.36, 34.28, 29.79, 27.06, 26.08, 25.43, 23.38, 22.13, 19.21. HR-MS (ESI)  $m/z$ : calculated for  $\text{C}_{33}\text{H}_{40}\text{F}_3\text{N}_3\text{O}_2$   $[\text{M}+\text{H}]^+$ : 568.3145, found: 568.3149.

**5.2.4.12. Methyl 12-N-3-(N-2, 6-dichlorobenzyl)indolosporidinolate dihydrochloride (6l).** Brown oil; Yield: 73%;  $^1\text{H}$  NMR (600 MHz, Chloroform-*d*)  $\delta$  7.72 (d,  $J = 7.9$  Hz, 1H), 7.46 (d,  $J = 8.1$  Hz, 1H), 7.37 (d,  $J = 8.0$  Hz, 2H), 7.23 (t,  $J = 7.9$  Hz, 2H), 7.11 (t,  $J = 7.5$  Hz, 1H), 6.78 (s, 1H), 5.46 (s, 2H), 3.66 (q,  $J = 8.4$ , 7.0 Hz, 5H), 3.06–2.91 (m, 3H), 2.85 (m, 1H), 2.58 (m, 2H), 2.45 (d,  $J = 8.4$  Hz, 1H), 2.25 (t,  $J = 7.2$  Hz, 2H), 2.11–1.90 (m, 3H), 1.86 (m, 1H), 1.80–1.32 (m, 8H), 1.27 (m, 2H), 1.05 (m, 1H).  $^{13}\text{C}$  NMR (151 MHz,  $\text{CDCl}_3$ )  $\delta$  173.88, 137.19, 136.85, 132.25 (2), 130.11, 128.75 (2), 128.10, 125.82, 121.68, 120.23, 118.95, 113.52, 109.49, 62.86, 59.37, 54.34, 51.52, 51.47, 50.20, 45.46, 44.92, 37.93, 34.24, 29.35, 27.33, 25.57, 24.99, 23.24, 21.97, 19.10. HR-MS (ESI)  $m/z$ : calculated for  $\text{C}_{32}\text{H}_{39}\text{Cl}_2\text{N}_3\text{O}_2$   $[\text{M}+\text{H}]^+$ : 568.2492, found: 568.2491.

**5.2.4.13. Methyl 12-N-3-(N-2-naphthyl) indolosporidinolate dihydrochloride (6m).** Yellow oil; Yield: 68%;  $^1\text{H}$  NMR (600 MHz, Chloroform-*d*)  $\delta$  7.88–7.70 (m, 4H), 7.58 (s, 1H), 7.50–7.42 (m, 2H), 7.32 (d,  $J = 8.2$  Hz, 1H), 7.26 (m, 1H), 7.21–7.16 (m, 1H), 7.16–7.11 (m, 1H), 7.05 (s, 1H), 5.45 (s, 2H), 3.78–3.72 (m, 2H), 3.67 (s, 3H), 3.12 (m, 1H), 3.06–2.91 (m, 3H), 2.74–2.64 (m, 2H), 2.61–2.50 (m, 1H), 2.40–2.26 (m, 2H), 2.15–2.02 (m, 3H), 1.95 (m, 1H), 1.84–1.44 (m, 9H), 1.42–1.32 (m, 2H), 1.11 (m, 1H).  $^{13}\text{C}$  NMR (151 MHz,  $\text{CDCl}_3$ )  $\delta$  174.02, 137.18, 135.12, 133.32, 132.82, 128.62, 128.38, 127.76, 127.71, 127.18, 126.35, 126.02, 125.65, 124.90, 121.82, 120.33, 119.01, 113.66, 109.60, 63.39, 58.89, 53.44, 51.49, 51.19, 50.34, 50.11, 45.03, 37.43, 34.21, 28.90, 27.58, 24.82, 24.66, 23.28, 22.01, 18.94. HR-MS (ESI)  $m/z$ : calculated for  $\text{C}_{36}\text{H}_{43}\text{N}_3\text{O}_2$   $[\text{M}+\text{H}]^+$ : 550.3428, found: 550.3428.

**5.2.4.14. Methyl 12-N-3-(5-fluoro-N-4-chlorobenzyl) indolosporidinylate dihydrochloride (6n).** Yellow oil; Yield: 76%;  $^1\text{H}$  NMR (600 MHz, Chloroform-*d*)  $\delta$  7.38 (m, 1H), 7.22–7.19 (m, 2H), 7.04 (m, 1H), 7.00–6.94 (m, 3H), 6.85 (m, 1H), 5.16 (s, 2H), 3.66 (d,  $J = 2.2$  Hz, 2H), 3.62 (s, 3H), 3.02–2.89 (m, 3H), 2.85–2.79 (m, 1H), 2.57 (m, 1H), 2.51 (m, 1H), 2.45–2.39 (m, 1H), 2.31–2.21 (m, 2H), 2.10–1.90 (m, 3H), 1.86–1.36 (m, 9H), 1.30–1.21 (m, 2H), 1.10–1.00 (m, 1H).  $^{13}\text{C}$  NMR (151 MHz,  $\text{CDCl}_3$ )  $\delta$  173.84, 157.51 (d,  $J = 234.2$  Hz), 135.96, 133.45, 128.89 (2), 128.57, 128.06 (2), 113.81, 113.78, 110.15, 110.09, 105.43, 105.27, 63.09, 59.33, 54.52, 51.73, 51.43, 50.23, 49.50, 45.52, 38.12, 34.18, 29.55, 27.16, 25.83, 25.22, 23.28, 21.95, 19.13. HR-MS (ESI)  $m/z$ : calculated for  $\text{C}_{32}\text{H}_{39}\text{ClFN}_3\text{O}_2$   $[\text{M}+\text{H}]^+$ : 552.2788, found: 552.2791.

**5.2.4.15. Methyl 12-N-3-(5-fluoro-N-4-trifluoromethylbenzyl) indolosporidinylate dihydrochloride (6o).** Yellow oil; Yield: 78%;  $^1\text{H}$  NMR (600 MHz, Chloroform-*d*)  $\delta$  7.53 (d,  $J = 8.1$  Hz, 2H), 7.34 (m, 1H), 7.16 (d,  $J = 8.0$  Hz, 2H), 7.10–7.04 (m, 2H), 6.90 (m, 1H), 5.32 (s, 2H), 3.75–3.67 (m, 2H), 3.65 (s, 3H), 3.35–3.26 (m, 2H), 3.21 (m, 1H), 3.11 (m, 1H), 3.00 (m, 1H), 2.69–2.60 (m, 2H), 2.40–2.24 (m, 3H), 2.22–1.62 (m, 9H), 1.47–1.39 (m, 2H), 1.25–1.13 (m, 1H).  $^{13}\text{C}$  NMR (151 MHz,  $\text{CDCl}_3$ )  $\delta$  173.82, 157.62 (d,  $J = 234.9$  Hz), 141.38, 133.53, 130.01 (q,  $J = 32.4$  Hz), 128.94, 128.57, 126.88 (2), 125.77 (2), 125.76, 113.05, 110.52, 110.25, 105.18, 62.45, 59.98, 52.88, 51.48, 50.77, 49.91, 49.75, 45.26, 35.96, 33.83, 28.58, 27.24, 23.31, 22.90 (2), 21.60, 18.44. HR-MS (ESI)  $m/z$ : calculated for  $\text{C}_{33}\text{H}_{39}\text{F}_4\text{N}_3\text{O}_2$   $[\text{M}+\text{H}]^+$ : 586.3051, found: 586.3057.

**5.2.4.16. Methyl 12-N-3-(5-fluoro-N-2, 6-dichlorobenzyl) indolosporidinylate dihydrochloride (6p).** Brown oil; Yield: 71%;  $^1\text{H}$  NMR (600 MHz, Chloroform-*d*)  $\delta$  7.43–7.37 (m, 3H), 7.31 (m, 2H), 7.00 (m, 1H), 6.85 (s, 1H), 5.49 (d,  $J = 3.0$  Hz, 2H), 3.69 (s, 5H), 3.40–3.31 (m, 2H), 3.25 (m, 1H), 3.17–3.04 (m, 2H), 2.64 (m, 2H), 2.50–2.43 (m, 1H), 2.40–2.12 (m, 6H), 2.12–1.99 (m, 2H), 1.94–0.79 (m, 8H).  $^{13}\text{C}$  NMR (151 MHz,  $\text{CDCl}_3$ )  $\delta$  173.72, 157.53 (d,  $J = 235.0$  Hz), 136.80 (2), 133.86, 131.88, 130.31, 128.86 (2), 128.18, 127.84, 112.47, 110.28, 110.23, 104.89, 62.17, 60.50, 53.12, 51.56, 50.51, 49.84, 45.52, 45.23, 35.86, 33.88, 29.70, 27.01, 23.06, 22.88, 22.70, 21.60, 18.37. HR-MS (ESI)  $m/z$ : calculated for  $\text{C}_{32}\text{H}_{38}\text{Cl}_2\text{FN}_3\text{O}_2$   $[\text{M}+\text{H}]^+$ : 586.2398, found: 586.2391.

### 5.2.5. General procedure for compound 9

**4a** (2 mmol) in  $\text{CH}_2\text{Cl}_2$  (10 mL) was added to  $(\text{Boc})_2\text{O}$  (2.2 mmol) and TEA (1 mL) and the mixture was stirred at room temperature. After 5 h, the organic solvent was concentrated in vacuo to produce **7**. Then  $\text{LiAlH}_4$  (4 mmol) was slowly added to the THF solution of **7** at  $0^\circ\text{C}$  and the solution was stirred for 2 h at room temperature. A solution of NaOH (10% in water) was then carefully added to the reaction mixture until a white solid precipitated. After filtration over  $\text{MgSO}_4$  and evaporation of the solvent, compound **8** in crude form was obtained. To a solution of **8** in  $\text{CH}_2\text{Cl}_2$  (15 mL),  $\text{NaHSO}_4 \cdot \text{SiO}_2$  (600 mg) was added and the mixture was refluxed. After completion of the reaction, the mixture was cooled and filtered. The concentrated filtrate was chromatographed over silica gel using a mixture of  $\text{CH}_2\text{Cl}_2$  and MeOH (5:1–3:1) to get **9**.

**5.2.5.1. 12-N-3-indolosporidinyl dihydrochloride (7).** White solid; Yield: 81%; Mp:  $77\text{--}79^\circ\text{C}$ ;  $^1\text{H}$  NMR (600 MHz, Chloroform-*d*)  $\delta$  8.24 (s, 1H), 7.78 (m, 1H), 7.37 (m, 1H), 7.21 (m, 1H), 7.13 (m, 1H), 7.07 (d,  $J = 2.3$  Hz, 1H), 3.77–3.72 (m, 2H), 3.61 (m, 2H), 3.02–2.89 (m, 3H), 2.79 (m, 1H), 2.68 (m, 1H), 2.52–2.43 (m, 2H), 2.11–2.01 (m, 3H), 1.85–1.72 (m, 3H), 1.68–1.48 (m, 6H), 1.44–1.26 (m, 3H), 1.21 (m, 2H), 1.07 (m, 1H).  $^{13}\text{C}$  NMR (151 MHz,  $\text{CDCl}_3$ )  $\delta$  136.66, 127.74, 122.82, 121.87, 120.19, 119.08, 114.90, 110.94, 63.99, 62.69, 59.14, 54.65, 51.52, 50.53, 45.51, 38.27, 33.10, 29.91, 26.99, 26.27, 25.53,

24.08, 22.09, 19.26. HR-MS (ESI)  $m/z$ : calculated for  $\text{C}_{24}\text{H}_{35}\text{N}_3\text{O}$   $[\text{M}+\text{H}]^+$ : 382.2853, found: 382.2858.

### 5.2.6. General procedure for compound 10a–10b

$\text{LiAlH}_4$  (2.0 equ.) was slowly added to the THF solution of ester (1.0 equiv) at  $0^\circ\text{C}$  and then the solution was stirred for 2 h at room temperature. After that, a solution of NaOH (10% in water) was carefully added until a white solid precipitated. After filtration over  $\text{MgSO}_4$  and evaporation of the solvent, the crude alcohol was purified by chromatography (silica gel,  $\text{CH}_2\text{Cl}_2/\text{MeOH}$ ) to give the pure product.

**5.2.6.1. 12-N-3-(N-benzyl)indolosporidinyl dihydrochloride (10a).** White solid; Yield: 94%; Mp:  $56\text{--}58^\circ\text{C}$ ;  $^1\text{H}$  NMR (600 MHz, Chloroform-*d*)  $\delta$  7.80 (d,  $J = 7.9$  Hz, 1H), 7.33–7.24 (m, 4H), 7.19 (m, 1H), 7.15–7.10 (m, 3H), 7.00 (d,  $J = 4.5$  Hz, 1H), 5.29 (d,  $J = 2.5$  Hz, 2H), 3.78–3.74 (m, 2H), 3.59 (t,  $J = 6.7$  Hz, 2H), 3.00–2.89 (m, 3H), 2.79 (m, 1H), 2.71–2.65 (m, 1H), 2.48 (m, 2H), 2.11–1.99 (m, 3H), 1.86–1.71 (m, 3H), 1.69–1.47 (m, 6H), 1.45–1.27 (m, 3H), 1.27–1.13 (m, 2H), 1.08 (m, 1H).  $^{13}\text{C}$  NMR (151 MHz,  $\text{CDCl}_3$ )  $\delta$  137.80, 137.06, 128.71 (2), 128.43, 127.52, 127.00, 126.76 (2), 121.69, 120.41, 118.88, 114.06, 109.50, 63.92, 62.45, 59.11, 54.58, 51.58, 50.45, 49.85, 45.47, 38.14, 33.15, 29.89, 27.06, 26.18, 25.48, 24.11, 22.00, 19.25. HR-MS (ESI)  $m/z$ : calculated for  $\text{C}_{31}\text{H}_{41}\text{N}_3\text{O}$   $[\text{M}+\text{H}]^+$ : 472.3322, found: 472.3324.

**5.2.6.2. 12-N-3-(N-4-bromobenzyl)indolosporidinyl dihydrochloride (10b).** White solid; Yield: 93%; Mp:  $72\text{--}74^\circ\text{C}$ ;  $^1\text{H}$  NMR (600 MHz, Chloroform-*d*)  $\delta$  7.80 (d,  $J = 7.8$  Hz, 1H), 7.45–7.40 (m, 2H), 7.23–7.17 (m, 2H), 7.13 (m, 1H), 7.01–6.95 (m, 3H), 5.23 (s, 2H), 3.76 (q,  $J = 13.4$  Hz, 2H), 3.60 (m, 2H), 3.02–2.87 (m, 3H), 2.79 (m, 1H), 2.68 (m, 1H), 2.48 (m, 2H), 2.14–1.98 (m, 3H), 1.87–1.72 (m, 3H), 1.70–1.48 (m, 6H), 1.48–1.27 (m, 3H), 1.27–1.15 (m, 2H), 1.09 (m, 1H).  $^{13}\text{C}$  NMR (151 MHz,  $\text{CDCl}_3$ )  $\delta$  136.92, 136.84, 131.84 (2), 128.48, 128.42 (2), 126.78, 121.87, 121.40, 120.52, 119.08, 114.42, 109.38, 63.92, 62.45, 59.06, 54.57, 51.62, 50.42, 49.30, 45.46, 38.09, 33.16, 29.90, 27.05, 26.18, 25.49, 24.12, 21.99, 19.25. HR-MS (ESI)  $m/z$ : calculated for  $\text{C}_{31}\text{H}_{40}\text{BrN}_3\text{O}$   $[\text{M}+\text{H}]^+$ : 550.2428, found: 550.2424.

### 5.3. In vitro cytotoxicity assay

The HepG2, CNE-2 and A549 cell lines were obtained from American Type Culture Collection (ATCC). The suspension (100  $\mu\text{L}$ /well) with evaluated cells ( $3\text{--}4 \times 10^4$  cell/mL) and DMEM culture medium of 10% fetal bovine serum (FBS) was seeded into 96-well plates. After a 24 h incubation period in 5%  $\text{CO}_2$ , compounds with different concentrations (1, 5, 10, 20, 50  $\mu\text{M}$ ), made by serial dilution in culture medium (DMEM of 10% fetal bovine serum) of stock solutions of test compounds prepared in DMSO, were added and in incubation for 48 h. Final concentration of DMSO was less than 0.1% in each well. Then 20  $\mu\text{L}$  of 5 mg/mL MTT (3-(4,5-dimethylthiazol-2-yl)-2,5-diphenyltetrazolium bromide) (Sigma, St. Louis, MO, USA) was added to each well, followed by incubation for 4 h at  $37^\circ\text{C}$ . Supernatant from each well was carefully removed and 150  $\mu\text{L}$  DMSO was added to each well for the colorimetric reaction. Finally, the optical density was measured at the 490 nm wavelength on an enzyme-linked immunosorbent assay microplate reader and each concentration was tested in threefold.

### 5.4. Topo I inhibitory activity

Topo I enzymatic activity was determined by measuring the decreased mobility of the relaxed isomers of supercoiled pBR322 DNA. Topo I and pBR322 were purchased from Takara Bio Inc. One unit of enzyme was defined as the amount that completely relaxes

0.5 µg of supercoiled pBR322 DNA in 30 min at 37 °C. The assay was performed in a final volume of 20 mL reaction volume containing 0.5 µg pBR322 DNA and 1 unit of human Topo I with or without our compounds in the reaction buffer. The mixture was continued to incubate at 37 °C for 30 min and then was terminated by adding 0.5% SDS, 0.25 µg/mL bromophenol blue, and 15% glycerol and the reaction products were separated on a horizontal 0.8% agarose gel in 1 × tris-acetate/EDTA buffer at 4 V/cm for 40 min at room temperature. The gel was stained with 5 µg/mL ethidium bromide and imaging was conducted by Gel Documentation system (Bio-Rad, USA).

### 5.5. Cell cycle arrest

HepG2 cells were seeded into a 6-well plate at  $2 \times 10^5$  cells per well. The cells were incubated in DMEM culture medium supplemented with 10% FBS and then treated with 10b at concentrations of 1, 2.5, and 5 µmol/L for 24 h. Then the cells were harvested and fixed in cold 75% ethanol at 4 °C overnight. After washing with PBS, the cells were incubated with 100 mg/mL RNase at 37 °C for 30 min. Subsequently, the cells were incubated with 50 mg/mL propidium iodide in the dark for 30 min. Then, the stained cells were analyzed by flow cytometry.

### 5.6. In vivo antitumor activity of 10b against HepG2 cells

This study was approved by the SPF Animal Laboratory of Guangxi University. Female BALB/c nude mice with five-to six-week-old were purchased from Beijing Vital River Laboratory Animal Technology Co., Ltd. (Beijing, China). The mice were maintained in air-conditioned rooms under controlled lighting (12 h light/day) and were fed with standard laboratory food and water. Tumor cell line xenografts were established by subcutaneously injection of HepG2 cells ( $8 \times 10^6$ ) into the flanks of the mice. Tumor sizes were determined using micrometer calipers. When tumors were ~150–200 mm<sup>3</sup>, mice were randomly assigned into four groups and treated with saline containing 10% DMSO (vehicle control, n = 6), sophoridine (40 mg/kg, n = 5), compound 10b (40 mg/kg, n = 5) and positive control irinotecan (40 mg/kg, n = 5) by intraperitoneal injection twice a week, respectively [39]. All of the animals were treated for 25 days. Tumor sizes were measured every other day. At the end of treatment, the tumor tissues were harvested, weighed and photographed. Tumor volume was calculated by the formula: tumor volume =  $0.5 \times \text{Length (L)} \times \text{Width (W)}^2$ . Tumor growth inhibition =  $\Delta T/\Delta C \times 100\%$ ; ( $\Delta T$  = tumor volume change in the treatment group on the final day of the study,  $\Delta C$  = tumor volume change in the control group on the final day of the study).

### Acknowledgements

This work was supported by the National Natural Science Foundation of China (21403225, 21402032), the high-level innovation team and outstanding scholar project of Guangxi institutions of higher education (guijiaoren (2014) 49 hao), the Guangxi Natural Science Foundation (2017GXNSFBA198240) and the State Key Laboratory for Chemistry and Molecular Engineering of Medicinal Resources, Guangxi Normal University (CMEMR2017-B14).

### Appendix A. Supplementary data

Supplementary data related to this article can be found at <https://doi.org/10.1016/j.ejmech.2018.07.028>.

### References

- [1] J.C. Wang, *Annu. Rev. Biochem.* 65 (1996) 635–692.
- [2] J.J. Champoux, In DNA topology and its biological effects, in: J.C. Wang, N.R. Cozzarelli (Eds.), Cold Spring Harbor Laboratory Press, Cold Spring Harbor, NY, 1990, pp. 217–242.
- [3] Y.D.N.A. Prommer, *Topoisomerases and Cancer*, first ed., Springer, 2012.
- [4] I. Husain, J.L. Mohler, H.F. Seigler, J.M. Besterman, Elevation of topoisomerase I messenger RNA, protein, and catalytic activity in human tumors: demonstration of tumor-type specificity and implications for cancer chemotherapy, *Cancer Res.* 54 (1994) 539–546.
- [5] T.D. Pfister, W.C. Reinhold, K. Agama, S. Gupta, S.A. Khin, R.J. Kinders, R.E. Parchment, J.E. Tomaszewski, J.H. Doroshow, Y. Pommier, Mol, Topoisomerase I levels in the NCI-60 cancer cell line panel determined by validated ELISA and microarray analysis and correlation with indenoisoquinoline sensitivity, *Canc. Ther.* 8 (2009) 1878–1884.
- [6] W.C. Reinhold, J.L. Mergny, H. Liu, M. Ryan, T.D. Pfister, R. Kinders, R. Parchment, J. Doroshow, J.N. Weinstein, Y. Pommier, Exon array analyses across the NCI-60 reveal potential regulation of TOP1 by transcription pausing at guanosine quartets in the first intron, *Cancer Res.* 70 (2010) 2191–2203.
- [7] G. Giaccone, J. van Ark-Otte, G. Scagliotti, G. Capranico, P. van der Valk, G. Rubio, O. Dalesio, R. Lopez, F. Zunino, J. Walboomers, et al., Differential expression of DNA topoisomerases in non-small cell lung cancer and normal lung, *Biochim. Biophys. Acta* 1264 (1995) 337–346.
- [8] Y. Pommier, DNA topoisomerase I inhibitors: chemistry, biology, and interfacial inhibition, *Chem. Rev.* 109 (2009) 2894–2902.
- [9] B.C. Giovanella, J.S. Stehlin, M.E. Wall, M.C. Wani, A.W. Nicholas, L.F. Liu, R. Silber, M. Potmesil, DNA topoisomerase I-targeted chemotherapy of human colon cancer in xenografts, *Science* 246 (1989) 1046–1048.
- [10] M. Brangi, T. Litman, M. Ciotti, K. Nishiyama, G. Kohlhagen, C. Takimoto, R. Robey, Y. Pommier, T. Fojo, S.E. Bates, Camptothecin resistance: role of the ATP-binding cassette (ABC), mitoxantrone-resistance half-transporter (MXR), and potential for glucuronidation in MXR-expressing cells, *Cancer Res.* 59 (1999) 5938–5946.
- [11] D.J. Adams, M.W. Dewhirst, J.L. Flowers, M.P. Gamcsik, O.M. Colvin, G. Manikumar, M.C. Wani, M.E. Wall, Camptothecin analogs with enhanced antitumor activity at acidic pH, *Cancer Chemother. Pharmacol.* 46 (2000) 263–271.
- [12] R.P. Hertzberg, M.J. Caranfa, K.G. Holden, D.R. Jakas, G. Gallagher, M.R. Mattern, S.M. Mong, J.O. Bartus, R.K. Johnson, W.D. Kingsbury, Modification of the hydroxyl lactone ring of camptothecin: inhibition of mammalian topoisomerase I and biological activity, *J. Med. Chem.* 32 (1989) 715–720.
- [13] M.E. Wall, M.C. Wani, *Cancer Res.* 55 (1995) 753–760.
- [14] Y. Pommier, *Chem. Rev.* 109 (2009) 2894–2902.
- [15] C.Q. Sheng, Z.Y. Miao, W.N. Zhang, *Curr. Med. Chem.* 18 (2011) 4389–4409.
- [16] W.M. Bonner, C.E. Redon, J.S. Dickey, A.J. Nakamura, O.A. Sedelnikova, S. Solier, Y. Pommier, *Nat. Rev. Canc.* 8 (2008) 957–967.
- [17] B.H. Long, W.C. Rose, D.M. Vyas, J.A. Matson, S. Forenza, *Curr. Med. Chem. Anticancer Agents* 2 (2002) 255–266.
- [18] B.L. Staker, M.D. Feese, M. Cushman, Y. Pommier, D. Zembower, L. Stewart, A.B. Burgin, *J. Med. Chem.* 48 (2005) 2336–2345.
- [19] G. Ye, H.Y. Zhu, Z.X. Li, C.H. Ma, M.S. Fan, Z.L. Sun, C.G. Huang, LC-MS characterization of efficacy substances in serum of experimental animals treated with *Sophora flavescens* extracts, *Biomed. Chromatogr.* 21 (2007) 655–660.
- [20] Y.M. Li, G. Min, Q. Xue, L. Chen, W. Liu, H. Chen, High performance liquid chromatographic method for simultaneous determination of sophoridine and matrine in rat plasma, *Biomed. Chromatogr.* 18 (2004) 619–624.
- [21] P.Y. Hu, Q. Zheng, H. Chen, Z.F. Wu, P.F. Yue, M. Yang, Pharmacokinetics and distribution of sophoridine nanoliposomes in rats, *Zhongguo Xinyao Zazhi* 21 (2012) 2662–2666.
- [22] Y. Wei, X. Wu, X. Liu, J. Luo, A rapid reversed phase highperformance liquid chromatographic method for determination of sophoridine in rat plasma and its application to pharmacokinetics studies, *J. Chromatogr. B: Anal. Technol. Biomed. Life Sci.* 843 (2006) 10–14.
- [23] C.W. Bi, N. Zhang, P. Yang, C. Ye, Y.X. Wang, T.Y. Fan, R.G. Shao, H.B. Deng, D.Q. Song, Synthesis, biological evaluation, and autophagy mechanism of 12 N-substituted sophoridinamines as novel anticancer agents, *ACS Med. Chem. Lett.* 8 (2017) 245–250.
- [24] C.J. Tan, Y. Zhao, M. Goto, K.Y. Hsieh, X.M. Yang, S.L. Morris-Natschke, L.N. Liu, B.Y. Zhao, K.H. Lee, *Bioorg. Med. Chem. Lett.* 26 (2016) 1495–1497.
- [25] D.D. Li, L.L. Dai, N. Zhang, Z.W. Tao, Synthesis, structure–activity relationship and biological evaluation of novel nitrogen mustard sophoridinic acid derivatives as potential anticancer agents, *Bioorg. Med. Chem. Lett.* 25 (2015) 4092–4096.
- [26] R. Pandey, K.V. Swamy, M.B. Khetmalas, Indole: a novel signaling molecule and its applications, *Indian J. Biotechnol.* 12 (2013) 297–310.
- [27] T. James, P. Maclellan, G.M. Burslem, I. Simpson, J.A. Grant, S. Warriner, V. Sridharan, A. Nelson, A modular lead-oriented synthesis of diverse piperazine, 1,4-diazepane and 1,5-diazocane scaffolds, *Org. Biomol. Chem.* 12 (2014) 2584–2591.
- [28] R.R. Kondreddi, J. Jiricek, S.P. Rao, S.B. Lakshminarayana, L.R. Camacho, R. Rao, M. Herve, P. Bifani, N.L. Ma, K. Kuhlen, A. Goh, A.K. Chatterjee, T. Dick, T.T. Diagona, U.H. Manjunatha, P.W. Smith, Design, synthesis, and biological evaluation of indole-2-carboxamides: a promising class of antituberculosis

- agents, *J. Med. Chem.* 56 (2013) 8849–8859.
- [29] A.S. da Silva Guerra, D.J. do Nascimento Malta, L.P. Morais Laranjeira, M.B. Souza Maia, N.C. Cavalcanti Colaco, M. do Carmo Alves de Lima, S.L. Galdino, I. da Rocha Pitta, T. Goncalves-Silva, Anti-inflammatory and antinociceptive activities of indole-imidazolidine derivatives, *Int. Immunopharmacol.* 11 (2011) 1816–1822.
- [30] Q.V. Vo, C. Trenerry, S. Rochfort, J. Wadeson, C. Leyton, A.B. Hughes, Synthesis and anti-inflammatory activity of indole glucosinolates, *Bioorg. Med. Chem.* 22 (2014) 856–864.
- [31] J.A. Caruso, R. Campana, C. Wei, C.H. Su, A.M. Hanks, W.G. Bornmann, K. Keyomarsi, Indole-3-carbinol and its N-alkoxy derivatives preferentially target ERalpha-positive breast cancer cells, *Cell Cycle* 13 (2014) 2587–2599.
- [32] S.A. Patil, R. Patil, D.D. Miller, Indole molecules as inhibitors of tubulin polymerization: potential new anticancer agents, *Future Med. Chem.* 4 (2012) 2085–2115.
- [33] T. Saini, S. Kumar, B. Narasimhan, Central nervous system activities of indole derivatives: an overview, *Cent. Nerv. Syst. Agents Med. Chem.* 16 (2015) 19–28.
- [34] A.A. Bekhit, O.A. El-Sayed, E. Aboulmagd, J.Y. Park, Tetrazolo[1,5-a]quinoline as a potential promising new scaffold for the synthesis of novel anti-inflammatory and antibacterial agents, *Eur. J. Med. Chem.* 39 (2004) 249–255.
- [35] X. Li, W.L. Zhao, J.D. Jiang, K.H. Ren, N.N. Du, Y.B. Li, Y.X. Wang, C.W. Bi, R.G. Shao, D.Q. Song, Synthesis, structure–activity relationship and biological evaluation of anticancer activity for novel N-substituted sophoridinic acid derivatives, *Bioorg. Med. Chem. Lett* 21 (2011) 5251–5254.
- [36] Z.G. Yuan, S.P. Chen, C.J. Chen, J.W. Chen, C.K. Chen, Q.Z. Dai, C.M. Gao, Y.Y. Jiang, Design, synthesis and biological evaluation of 4-amidobenzimidazole acridine derivatives as dual PARP and Topo inhibitors for cancer therapy, *Eur. J. Med. Chem.* 138 (2017) 1135–1146.
- [37] P. D'Arpa, C. Beardmore, L.F. Liu, Involvement of nucleic acid synthesis in cell killing mechanisms of topoisomerase poisons, *Cancer Res.* 50 (1990) 6919–6924.
- [38] M.K. Gofar, N.A. Rayeni, S. Rasouli, Topoisomerase inhibitors and types of them, *Int. J. Biol. Med. Res.* 2 (2014) 2431–2436.
- [39] J.L. Zou, S. Li, Z.H. Chen, Z.H. Lu, J. Gao, J.Y. Zou, X.T. Lin, Y.Y. Li, C. Zhang, L. Shen, A novel oral camptothecin analog, gimitecan, exhibits superior antitumor efficacy than irinotecan toward esophageal squamous cell carcinoma *in vitro* and *in vivo*, *Cell Death Dis.* 9 (2018) 661.